that up-regulation of hepatic ISGs in treatment-resistant IL28B genotype patients was mediated by multiple factors, including IL28A/B, IFN-λ4, and WNT5A. We found a significant negative correlation between WNT5A and various chemokines in liver of CHC patients (Supporting Fig. 7). Interestingly, WNT5A directly repressed one of these chemokines, CXCL13, a B-lymphocyte chemoattractant, in HCV-infected hepatocytes. These results indicate that loss of immune cells from the liver may be associated with the induction of other inflammatory factors, such as WNT5A, in MI patients, although we did not identify which cells express WNT5A. Further studies are needed to explore their functional relevance in the pathogenesis of CHC.

Acknowledgment: The authors thank Mina Nishiyama for her technical assistance.

References

1. Fried MW, Shiffman ML, Reddy KR, Smith C, Marinos G, Goncales FL, Jr., et al. Peginterferon alfa-2a plus ribavirin for chronic hepatitis C virus infection. N Engl J Med 2002;347:975-982.
2. Zeuzem S, Andreone P, Pol S, Lawitz E, Diago M, Roberts S, et al. Telaprevir for retreatment of HCV infection. N Engl J Med 2011;364:2417-2428.
3. Ge D, Fellay J, Thompson AJ, Simon JS, Shianna KV, Urban TJ, et al. Genetic variation in IL28B predicts hepatitis C treatment-induced viral clearance. Nature 2009;461:399-401.
4. Suppiah V, Moldovan M, Ahlenstiel G, Berg T, Weltman M, Abate ML, et al. IL28B is associated with response to chronic hepatitis C interferon-alpha and ribavirin therapy. Nat Genet 2009;41:1100-1104.
5. Tanaka Y, Nishida N, Sugiyama M, Kurosaki M, Matsuura K, Sakamoto N, et al. Genome-wide association of IL28B with response to pegylated interferon-alpha and ribavirin therapy for chronic hepatitis C. Nat Genet 2009;41:1105-1109.
6. Honda M, Sakai A, Yamashita T, Nakamoto Y, Mizukoshi E, Sakai Y, et al. Hepatic ISG expression is associated with genetic variation in interleukin 28B and the outcome of IFN therapy for chronic hepatitis C. Gastroenterology 2010;139:499-509.
7. Honda M, Nakamura M, Tateno M, Sakai A, Shimakami T, Shirasaki T, et al. Differential interferon signaling in liver lobule and portal area cells under treatment for chronic hepatitis C. J Hepatol 2010;53:817-826.
8. Prokunina-Olsson L, Muchmore B, Tang W, Pfeiffer RM, Park H, Dickensheets H, et al. A variant upstream of IFNL3 (IL28B) creating a new interferon gene IFNL4 is associated with impaired clearance of hepatitis C virus. Nat Genet 2013;45:164-171.
9. Wakita T, Pietschmann T, Kato T, Date T, Miyamoto M, Zhao Z, et al. Production of infectious hepatitis C virus in tissue culture from a cloned viral genome. Nat Med 2005;11:791-796.
10. Garaigorta U, Heim MH, Boyd B, Wieland S, Chisari FV. Hepatitis C virus (HCV) induces formation of stress granules whose proteins regulate HCV RNA replication and virus assembly and egress. J Virol 2012;86:11043-11056.
11. Bikkavilli RK, Malbon CC. Arginine methylation of G3BP1 in response to Wnt3a regulates beta-catenin mRNA. J Cell Sci 2011;124:2310-2320.
12. Sarasin-Filipowicz M, Oakeley EJ, Duong FH, Christen V, Terracciano L, Filipowicz W, Heim MH. Interferon signaling and treatment outcome in chronic hepatitis C. Proc Natl Acad Sci U S A 2008;105:7034-7039.
13. Chen L, Borozan I, Feld J, Sun J, Tannis LL, Coltescu C, et al. Hepatic gene expression discriminates responders and nonresponders in treatment of chronic hepatitis C viral infection. Gastroenterology 2005;128:1437-1444.
14. Kudo S, Matsuno K, Ezaki T, Ogawa M. A novel migration pathway for rat dendritic cells from the blood: hepatic sinusoids-lymph translocation. J Exp Med 1997;185:777-784.
15. Chen L, Borozan I, Sun J, Guindi M, Fischer S, Feld J, et al. Cell-type specific gene expression signature in liver underlies response to interferon therapy in chronic hepatitis C infection. Gastroenterology 2010;138:1123-1133.e1-3.
16. Askarieh G, Alsio A, Pugnale P, Negro F, Ferrari C, Neumann AU, et al. Systemic and intrahepatic interferon-gamma-inducible protein 10 kDa predicts the first-phase decline in hepatitis C virus RNA and overall viral response to therapy in chronic hepatitis C. HEPATOLOGY 2010;51:1523-1530.
17. Romanowska M, Evans A, Kellock D, Bray SE, McLean K, Donandt S, Foerster J. Wnt5a exhibits layer-specific expression in adult skin, is upregulated in psoriasis, and synergizes with type 1 interferon. PLoS One 2009;4:e5354.
18. Shapira SD, Gat-Viks I, Shum BO, Dricot A, de Grace MM, Wu L, et al. A physical and regulatory map of host-influenza interactions reveals pathways in H1N1 infection. Cell 2009;139:1255-1267.
19. Staal FJ, Luis TC, Tiemessen MM. WNT signalling in the immune system: WNT is spreading its wings. Nat Rev Immunol 2008;8:581-593.

Cellular Immunology 282 (2013) 44–52

Contents lists available at SciVerse ScienceDirect

Cellular Immunology

journal homepage: www.elsevier.com/locate/ycimm

ER stress induced impaired TLR signaling and macrophage differentiation of human monocytes

Takuya Komura [a,1], Yoshio Sakai [b,1], Masao Honda [a], Toshinari Takamura [a], Takashi Wada [b], Shuichi Kaneko [a,*]

[a] Disease Control and Homeostasis, Kanazawa University, 13-1, Takaramachi, Kanazawa 920-8641, Japan
[b] Department of Laboratory Medicine, Kanazawa University, 13-1, Takaramachi, Kanazawa 920-8641, Japan

ARTICLE INFO

Article history:
Received 10 September 2012
Accepted 14 April 2013
Available online 24 April 2013

Keywords:
ER stress
Monocyte
TLR signaling
Differentiation

ABSTRACT

Endoplasmic reticulum (ER) stress causes impairment of the intracellular protein synthesis machinery, affecting various organ functions and homeostasis systems, including immunity. We found that ER stress induced by the N-linked glycosylation inhibitor, tunicamycin, caused susceptibility to apoptosis in the human monocytic cell line, THP-1 cells. Importantly, prior to tunicamycin-induced apoptosis, the proinflammatory response to toll-like receptor (TLR) 4 ligand lipopolysaccharide (LPS) stimulation was attenuated with respect to the expression of the proinflammatory cytokines. This impaired expression of proinflammatory cytokines was a consequence of the inhibition of NF-κB activation. Moreover, tunicamycin-induced ER stress disturbed the differentiation of THP-1 cells into macrophages induced by phorbol-12-myristate-13-acetate treatment. We also confirmed that ER stress affected the response of primary human monocytes to TLR ligand and their ability to differentiate into macrophages. These data suggest that ER stress imposes an important pathological insult to the immune system, affecting the crucial functions of monocytes.

1. Introduction

Homeostasis of physiological activities and structural components of the body requires properly functioning cellular machinery, including the components involved in protein synthesis. The endoplasmic reticulum (ER) plays a central role in the synthesis, maturation and assembly of secretary and structural proteins [1], and under some conditions, ER stress can disrupt ER function [2]. ER stress affects physiological cellular activities, disturbing cell-type specific functions or cell viability and inducing apoptosis [3]. ER stress has been observed in a variety of diseases, such as cancer, metabolic diseases, atherosclerosis and neurodegenerative diseases, including Parkinson's disease and Alzheimer's disease [4–7]; however, it is not clear whether ER stress is the cause or consequence of these diseases.

Composed of many cell types, including monocytes, macrophages, dendritic cells (DCs) and lymphocytes, the immune system contributes to homeostasis by protecting the host from exogenous pathogens or harmful unexpected endogenous events, such as cancer. Monocytes are critical immune cells that express pattern-recognition molecules, toll-like receptors (TLRs), important for innate immunity against various pathogens [8,9]. Monocytes are also the progenitors for differentiation into macrophages or DCs, both of which are pivotal regulators of immune reaction [10].

Previously, we observed that human monocytes in patients with diabetes were under ER stress, were functionally impaired regarding TLR signaling and were vulnerable to apoptosis [11]. These observations suggested that ER stress is involved in the impairment of monocytes, thereby compromising host immunity.

In this study, we further examined how ER stress affects monocytes. When primary human monocytes and THP-1 human monocytic cell line cells were stimulated with toll-like receptor (TLR) 4 ligand lipopolysaccharide (LPS), we observed that monocytes were attenuated in their capability to secrete proinflammatory cytokines. Moreover, when cells were under ER stress induced by the N-linked glycosylation inhibitor, tunicamycin, decreased activation of NF-κB was observed. In addition to this functional impairment of cytokine expression, ER stress also impaired monocyte differentiation into macrophages. Interestingly, the TLR4 signaling in differentiated macrophages was also impaired under ER stress. These results demonstrate that ER stress is an important pathological condition that broadly affects monocyte-lineage cells, influencing the innate immune system function of monocytes and macrophages as well as the differentiation capability of progenitor cells for antigen presentation.

* Corresponding author. Address: Disease Control and Homeostasis, Graduate School of Medical Science, Kanazawa, University, Kanazawa 920-8641, Japan. Fax: +81 76 234 4250.
E-mail address: skaneko@m-kanazawa.jp (S. Kaneko).
[1] These authors contributed equally to this work.

0008-8749/$ - see front matter © 2013 Elsevier Inc. All rights reserved.
http://dx.doi.org/10.1016/j.cellimm.2013.04.006

2. Materials and methods

2.1. Human monocytes

THP-1 cells, a human monocytic cell line, were obtained from American Type Culture Collection (Manassas, VA). THP-1 cells were cultured in RPMI1640 culture medium (Invitrogen, Carlsbad, CA) supplemented with 10% heat-inactivated fetal bovine serum (FBS, Invitrogen). Human primary monocytes were obtained from healthy volunteers as follows: peripheral blood mononuclear cells (PBMCs) were freshly isolated from heparinized venous blood using Ficoll–Hypaque (Sigma–Aldrich, St. Louis, MO). $CD14^+$ monocyte subpopulations were isolated using a magnetic cell sorting system in accordance with the manufacturer's protocol (Miltenyi Biotec, Bergisch Gladbach, Germany).

2.2. Induction of macrophage-differentiation

For macrophage differentiation, THP-1 cells were cultured in medium supplemented with Phorbol-12-myristate-13-acetate (PMA) (50 ng/ml) (Sigma–Aldrich) for 72 h. Primary human monocytes were cultured in medium supplemented with GM-CSF (100 ng/ml) (Sigma–Aldrich) for 4 days. Macrophage differentiation was assessed by morphology under microscopic examination and expression of the macrophage-related surface markers, CD11b and CD68, as analyzed by flow cytometry analysis and quantitative real-time detection PCR (RTD-PCR).

2.3. ER stress induction

To induce ER stress, THP-1 cells were treated with 1 or 5 μg/ml of tunicamycin (Sigma–Aldrich) and 3 μM thapsigargin (Sigma–Aldrich) for 12 h. The treated cells were assessed for apoptosis and cytokine expression in response to LPS stimulation.

2.4. Flow cytometry analysis

Flow cytometry analysis was performed as previously reported. For the surface molecule expression, cells were incubated with phycoerythrin (PE)-labeled anti-TLR4 (eBioscience, San Diego, CA), anti- CD11b and CD68 (BD Biosciences, San Jose, CA) in PBS containing 2% bovine serum albumin (BSA) (Sigma–Aldrich). For assessment of apoptosis, cells were incubated with fluorescein isothiocyanate (FITC)-labeled anti-CD14 antibody (BD Bioscience) and with PE-labeled Annexin-V and 7-amino-actinomycin D (7-AAD, Apoptosis Detection Kit I, BD Biosciences). Apoptotic cells were determined by flow cytometry for the fraction of cells labeled with Annexin-V that were 7-AAD negative using a FACSCalibur™ flow cytometer (BD Biosciences). Data were analyzed using CELLQuest™ Software (BD Biosciences). At least 10,000 cells per sample were analyzed.

2.5. RTD-PCR

RTD-PCR was performed as previously described [12]. Briefly, total RNA obtained from cells using a MicroRNA isolation kit (Stratagene, La Jolla, CA) was reverse-transcribed using 1 μg oligo (dT) primer and Super Script II reverse transcriptase (Invitrogen) in accordance with the manufacturers' protocol. The relative quantities of mRNA expression were analyzed by RTD-PCR using an ABI PRISM 7900 HT Sequence Detection System (Applied Biosystems, Foster City, CA). Primer pairs and probes for BCL-2, BCL-XL, TLR4, MyD88, TNF-α, IL-1β, C/EBP homologous protein (CHOP), immunoglobulin heavy chain binding protein (BiP), CD11b, CD68, and β-actin were obtained from the TaqMan assay reagents library. Gene expression levels were calculated with the $2^{-\triangle\triangle Ct}$ method using β-actin as the internal control.

2.6. TLR ligand stimulation

LPS (1 μg/ml) from *E. coli* (Sigma–Aldrich) was added to conditioned THP-1 cells (3×10^5 cells) or PMA-induced differentiated cells in AIM-V culture medium (Invitrogen). After 3 h incubation, the gene expression of TNF-α and IL-1β was analyzed by RTD-PCR. In addition, the concentration of TNF-α and IL-1β in the culture medium supernatants after 12 h LPS stimulation was measured using an ELISA kit (eBioscience) in accordance with the manufacturer's protocol. With regard to primary human monocytes (5×10^5 cells), the gene expression of TNF-α and IL-1β was analyzed by RTD-PCR after 4 h LPS stimulation. The concentration of TNF-α and IL-1β in the culture medium supernatants after 12 h LPS stimulation was measured using an ELISA kit.

2.7. Measurement of caspase-3 activity

THP-1 cells (3×10^5) were harvested and treated with tunicamycin (5 μg/ml) in RPMI1640 culture medium. After 48 or 72 h incubation, THP-1 cells were lysed, and the DEVD-cleaving activity of active caspase-3 in the lysate was measured using labeled Asp-Glu-Val-Asp-p-nitroanilide (DEVD-pNA) as the substrate and the Caspase-3 Colorimetric Assay Kit (Promega, Madison, WI) in accordance with manufacturer's protocol. The *p*NA light emission was quantified using a microtiter plate reader at a wavelength of 405 nm.

2.8. Western blot

Conditioned THP-1cells were washed twice with PBS and lysed in 100 μl of lysis buffer (10 mM Tris–HCl (pH 7.4), 1% SDS). A total of 10 μg of total proteins were loaded per well and separated on a 7% SDS–PAGE by electrophoresis, followed by transfer to a nitrocellulose membrane. The transferred nitrocellulose membranes were probed with anti-TLR4, anti-MyD88 or anti-β-actin antibody (Cell Signaling Technology, Danvers, MA) at a concentration of 1:500. The secondary goat-anti-rabbit antibody conjugated with horseradish peroxidase (HRP) was used at a concentration of 1:1000 (Cell Signaling Technology). The membrane was visualized by chemiluminescence using the ECL kit (Amersham Biosciences, Piscataway, NJ). Each expression level was assessed and compared to β-actin expression using densitometry.

2.9. Microscopic observation of immunofluorescent cells

For assessment of NF-κB nuclear translocation, THP-1 cells were treated with tunicamycin for 12 h, followed by stimulation with LPS (1 μg/ml) for 40 min. Treated cells were plated at a density of 1×10^5 cells per 22-mm glass coverslip. Cells were fixed for 30 min in cold 4% paraformaldehyde, permeabilized for 2 min at 25 °C in 0.25% Triton X-100 and incubated with PBS supplemented with 10% BSA. Fixed and permeabilized cells were incubated with PBS with 10% BSA containing anti-NF-κB p65 (Cell Signaling Technology). After being washed three times in PBS, coverslips were incubated with the anti-rabbit IgG conjugated with FITC (Jackson Immunoresearch, West Grove, PA). Nuclei were stained with 4, 6-diamino-2-phenylindole (Vector Laboratories, Burlingame, CA). Fluorescent cells were examined with a laser-scanning confocal microscope (Radiance 2100; Bio-Rad, Hercules, CA).

2.10. NF-κB ELISA

Quantitative analysis of NF-κB p65 activation was performed using the CASE™ activation of signaling ELISA kit for NF-κB p65 S536 (SABiosciences Corporation, MD) according to the manufacturer's instructions with slight modifications. Briefly, 1.5×10^4 - cells were seeded and incubated on the 96-well plate overnight. Cells were fixed, washed and blocked to avoid non-specific antibody binding. Cells were incubated with anti-pan-NF-κB p65 S536 antibody or anti-phospho-NF-κB specific antibody, washed, and incubated with the secondary antibody. After washing cells, colorimetric detection was performed using a microtiter plate reader at a wavelength of 450 nm.

2.11. Statistical analysis

Data are expressed as means ± SEM. The Mann–Whitney *U* test was applied to assess the significant difference between the two groups. Statistical significance was determined as $P < 0.05$.

3. Results

3.1. Attenuation of TLR signaling prior to apoptosis in human monocytes under ER stress

We examined how ER stress affects the viability of THP-1 cells by assessing the frequency of apoptotic THP-1 cells when treated with tunicamycin (5 μg/ml). Apoptotic cells were defined as cells positive for Annexin-V and negative for 7-AAD by flow cytometry. As shown in Fig. 1A and B, a low frequency of apoptotic cells was observed at 12 h. After 24 h, an increased frequency of apoptosis was observed among THP-1 cells treated with tunicamycin compared to untreated cells. When cells were treated with tunicamycin for 48 h and 72 h, the activity of the pro-apoptotic protease, caspase-3, was significantly increased (Fig. 1C). Furthermore, the expression of the anti-apoptotic genes, BCL-2 and BCL-XL was substantially lower in tunicamycin-treated THP-1 cells compared with untreated cells (Fig. 1D). When cells were treated with tunicamycin, the activity of the pro-apoptotic protease caspase-3 was significantly increased after 48 h (Fig. 1C), though not at 12 h (data not shown). We also observed similar results using 1 μg/ml tunicamycin treatment, but alternations were less compared with 5 μg/ml tunicamycin treatment (data not shown). These results suggest that ER stress induced conventional apoptosis in the human monocytic cell line.

Monocytes typically express pattern-recognition molecules such as TLRs that are important for innate immunity against various pathogens. TLR4 is the receptor for the LPS ligand, and plays a role in host defense against gram-negative infection [13]. To determine whether THP-1 cells were functionally affected under ER stress induced by tunicamycin treatment, we assessed the responsiveness of THP-1 cells to LPS stimulation *in vitro*.

We examined whether the expression of TLR4 and MyD88, a crucial adaptor molecule for TLR signaling, was affected in THP-1 cells under ER stress induced by tunicamycin treatment at 12 h. We confirmed that tunicamycin treatment induced ER stress on THP-1 cells at 12 h, observing that the expression levels of pivotal genes related to ER stress, CHOP and BiP, were up-regulated (Fig. 2A). Whereas expression of TLR4 and MyD88 was not affected

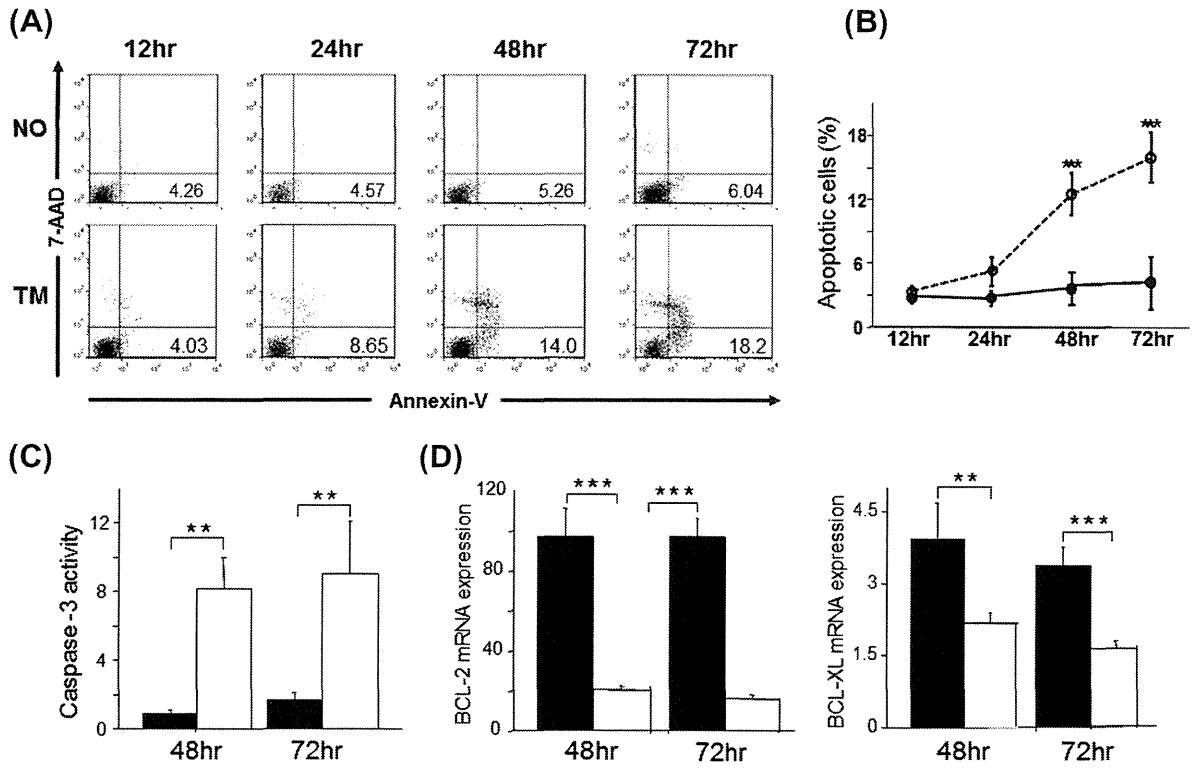

Fig. 1. ER stress increased the susceptibility of THP-1 cells to apoptosis. (A–B) THP-1 cells were incubated in culture medium supplemented with tunicamycin (5 μg/ml). The frequency of apoptotic cells was analyzed by flow cytometry at 12 h, 24 h 48 h and 72 h. More apoptotic cells were observed among the THP-1 cells treated with tunicamycin for more than 48 h incubation compared to the untreated THP-1 cells. (A) A representative scatter gram of Annexin-V and 7-AAD for THP-1 cells treated with tunicamycin. The numbers in each quadrant indicate the percentage of apoptotic cells. (B) The average number of apoptotic cells was calculated in triplicate for each condition. (C) Caspse-3 activity in THP-1 cells treated with tunicamycin was significantly increased at 48 h and 72 h incubation. (D) The BCL-2 and BCL-XL expressions in THP-1 cells incubated with tunicamycin for 48 h and 72 h were significantly down-regulated. Filled circle, no treatment; open circle, treatment with tunicamycin (5 μg/ml). TM, tunicamycin. Data are expressed as means ± SEM. $^{**}P < 0.01$, $^{***}P < 0.001$.

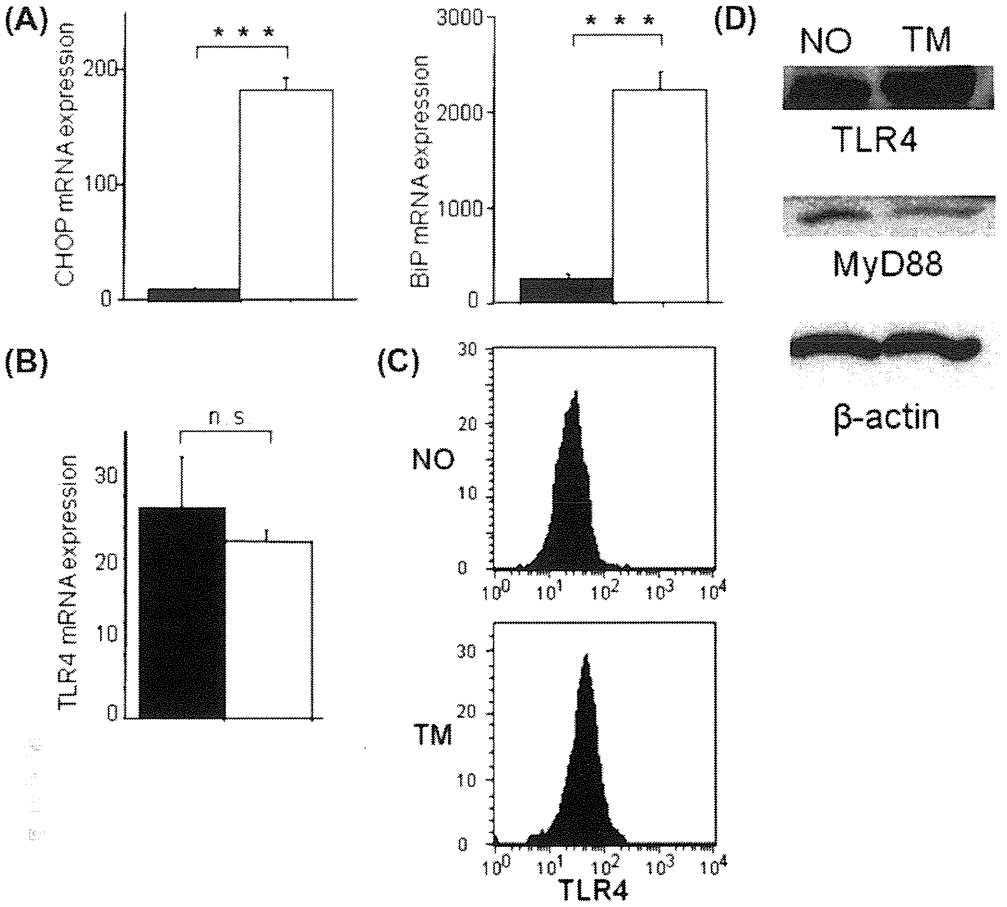

Fig. 2. Tunicamycin treatment induced ER-stress related molecules, but did not affect the expression of TLR4 and its accessory molecule MyD88 in THP-1 cells. (A) The transcriptional expression levels of the ER stress markers CHOP and BiP in THP-1 cells incubated with tunicamycin for 12 h were significantly up-regulated (RTD-PCR). Data are expressed as means ± SD of four independent experiments. (B–C) The expression of TLR4 was not affected by 12 h incubation with tunicamycin, as assessed by RTD-PCR (B), flow cytometry (C) and Western blot (D) Similarly, MyD88 expression was not affected (D). Filled bars, no treatment; open bars, treatment with tunicamycin (5 μg/ml). $^{***}P < 0.001$.

with 12 h incubation with tunicamycin (Fig. 2B–D), the gene expression of the proinflammatory cytokines, TNF-α and IL-1β, was down-regulated in the tunicamycin-treated THP-1 cells that were stimulated with LPS for 3 h (Fig. 3A). Concomitantly, the concentration of TNF-α and IL-1β in culture medium was also decreased after 12 h stimulation with LPS (Fig. 3B), indicating that the production of these cytokines from THP-1 cells was diminished. We also observed similar results using a lower concentration of tunicamycin (1 μg/ml), along with another ER stress inducer, thapsigargin, which is an endoplasmic reticulum Ca^{2+} ATPase inhibitor (Supplemental Fig. 1). Both 12 h tunicamycin (1 μg/ml) and 12 h thapsigargin (3 μM) treatments induced ER stress, but did not induce apoptosis, alteration of caspase-3 activity, or expression of anti-apoptotic genes (data not shown).Furthermore, we confirmed a similar effect of ER stress attenuation of TLR4 signaling in primary human monocytes (Fig. 3C and D). The gene expression of IL-1β was significantly down-regulated in tunicamycin-treated primary human monocytes that were stimulated with LPS for 4 h (Fig. 3C), and the gene expression of TNF-α was slightly down-regulated. The concentration of TNF-α and IL-1β in culture medium was also decreased after 12 h stimulation with LPS (Fig. 3D). These results demonstrate that TLR signaling in human monocytes under tunicamycin-induced ER stress was functionally impaired with regard to the TLR4 stimulation-signaling to produce proinflammatory cytokines.

3.2. ER stress inhibited the activation of NF-κB in THP-1 cells stimulated with LPS

To further assess how ER stress affects the expression of proinflammatory cytokines, we examined the expression of NF-κB, a pivotal transcriptional factor of proinflammatory cytokines [14,15]. THP-1 cells treated with tunicamycin were stimulated with LPS, and the activation of NF-κB was assessed every 40 min up to 120 min. Before LPS stimulation, no significant difference in NF-κB activation was observed, with or without treatment of tunicamycin in THP-1 cells (Fig. 4A). However, after LPS stimulation, NF-κB activation was not induced in THP-1 cells under ER stress compared with untreated THP-1 cells (Fig. 4A). Concomitantly, the translocation of NF-κB into the nucleus induced by LPS stimulation for 40 min was not observed in untreated THP-1 cells when cells were under ER stress (Fig. 4B). Furthermore, we examined the translocation of NF-κB induced by TNF-α stimulation in THP-1 cells under ER stress to clarify whether other stimulation also affects the activation of NF-κB under ER stress. We did not observed significant translocation of NF-κB following TNF-α stimulation, as compared with LPS stimulation (Supplemental Fig. 2), suggesting that the effect on NF-κB mobilisation under ER stress was caused only by TLR signaling. These results demonstrate that activation of NF-κB in response to the LPS stimulation was impaired in THP-1 cells under ER stress.

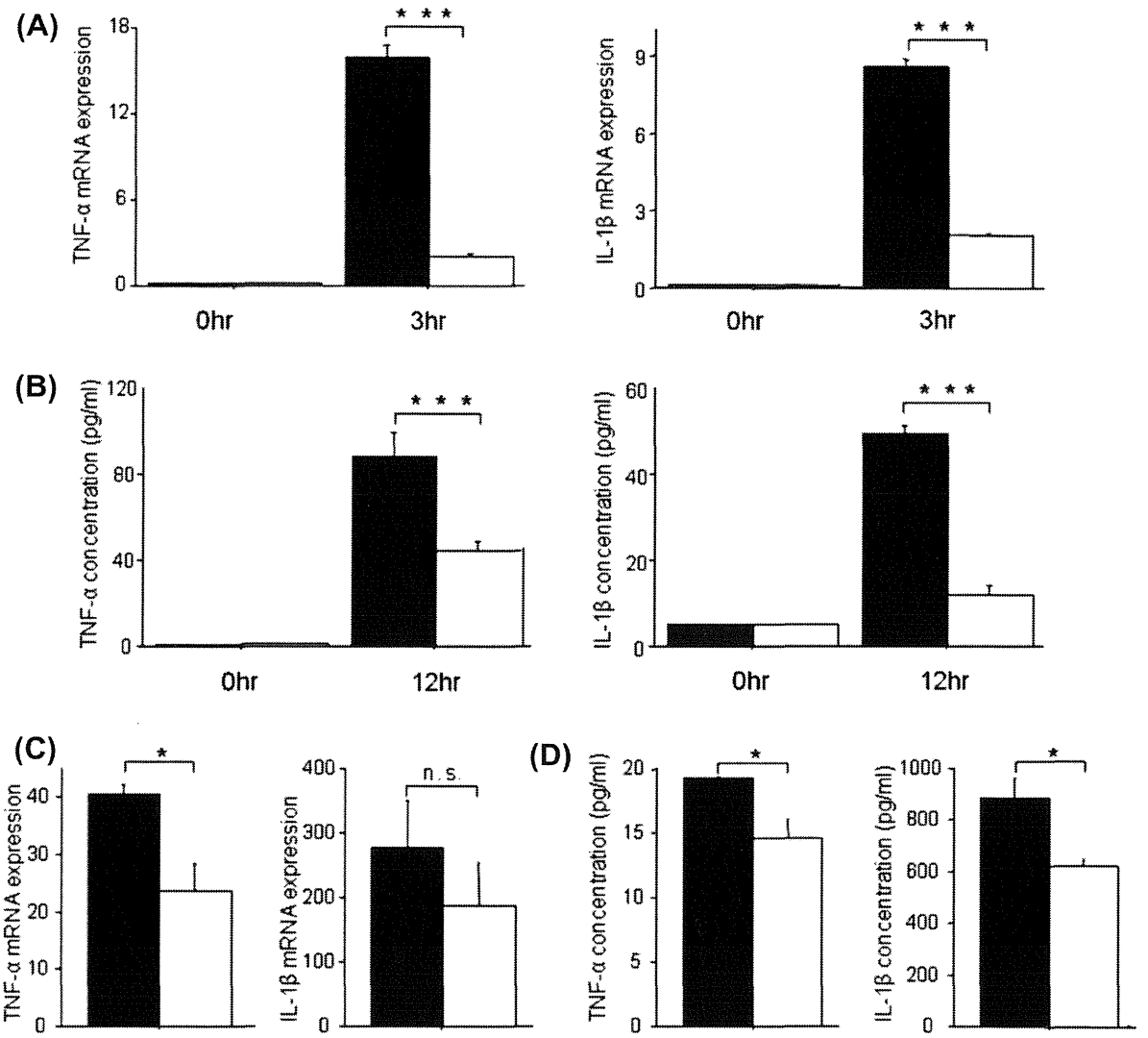

Fig. 3. Expression of proinflammatory cytokines in response to TLR ligand stimulation was decreased in human monocytes treated with tunicamycin. (A) THP-1 cells pretreated with tunicamycin (5 μg/ml) were cultured in AIM-V serum-free culture medium supplemented with LPS (1 μg/ml). After 3 h incubation with LPS, RNA was isolated from the THP-1 cells, and the expression levels of the TNF-α and IL-1β genes were analyzed by RTD-PCR. The expressions of these cytokines were down-regulated in THP-1 cells treated with tunicamycin. (B) THP-1 cells pretreated with tunicamycin were cultured in AIM-V serum-free culture medium supplemented with LPS (1 μg/ml) for 12 h and the concentration of TNF-α and IL-1β in the culture medium was measured by ELISA. The concentrations of these cytokines were decreased. (C) Primary human monocytes were cultured in AIM-V serum-free culture medium supplemented with LPS (1 μg/ml) and tunicamycin (5 μg/ml). After 4 h incubation, RNA was isolated from the cells, and the expression levels of the TNF-α and IL-1β genes was analyzed by RTD-PCR. The expression of IL-1β was down-regulated in cells treated with tunicamycin and TNF-α tended to be down-regulated. (D) Primary human monocytes were cultured in AIM-V serum-free culture medium supplemented with LPS (1 μg/ml) and tunicamycin (5 μg/ml) for 12 h, and the concentration of TNF-α and IL-1β in the culture medium was measured by ELISA. The concentration of these cytokines was decreased. Data are expressed as means ± SEM of four independent experiments. Filled bars; no treatment. Open bar; treatment with tunicamycin (5 μg/ml). $^{*}P < 0.05$, $^{***}P < 0.001$.

3.3. ER stress impaired monocyte differentiation into macrophages

Monocytes are progenitor cells that differentiate into macrophages and play an important role for inducing acquired immunity [16]. We tried to differentiate THP-1 cells and primary human monocytes into macrophages by PMA and GM-CSF treatment, respectively. When THP-1 cells were treated with PMA for 3 days, cells appeared morphologically mature, showing increased forward scatter (FSC) and side scatter (SSC) (Fig. 5A and B), and displayed enhanced expression of the macrophage-related markers CD11b and CD68 by flow cytometry (Fig. 5C). However, when THP-1 cells were pretreated with tunicamycin followed by PMA treatment, no alteration of FSC and SSC was observed (Fig. 5A and B) and the expression levels of CD11b and CD68 (Fig. 5C and D) were not enhanced. We confirmed that the ER stress markers CHOP and BiP were upregulated in the PMA-differentiated THP-1 cells with tunicamycin treatment (Fig. 5E). Furthermore, when primary human monocytes were treated with or without tunicamycin and cultured in media with GM-CSF for 4 days, tunicamycin-treated primary human monocytes showed less mature morphological appearance (Fig. 5F), lower FSC and SSC (Fig. 5G) and lower CD11b expression (Fig. 5H) compared to those of untreated primary human monocytes. In THP-1 cells, the differentiated cells under ER stress showed the same expression levels of TLR and MyD88 regardless of tunicamycin-induced ER stress (Fig. 6A and B). However, TNF-α and IL-1β expression levels were significantly decreased in differentiation-induced THP-1 cells under ER stress (Fig. 6C and D). These results suggest that tunicamycin-induced ER stress disturbed the differentiation capability as well as the signaling pathway of TLR4 in monocytes.

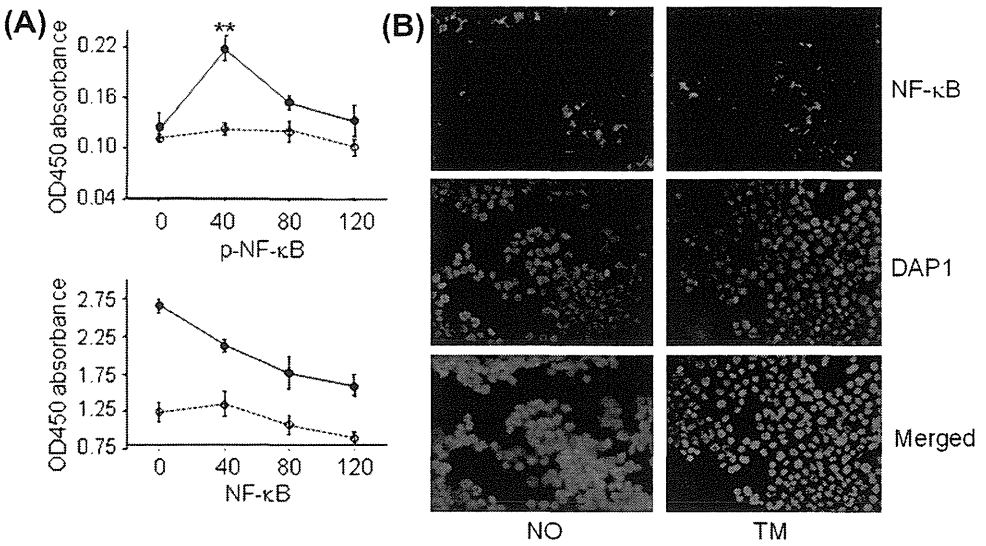

Fig. 4. NF-κB activation in response to LPS stimulation in human monocytes was attenuated under ER stress. (A) THP-1 cells treated with tunicamycin (5 μg/ml) for 12 h were cultured in AIM-V serum-free medium supplemented with LPS. Phosphorylated or total NF-κB quantity in THP-1 cells seeded on the culture plate was assessed by cellular activation of the signaling ELISA kit. Induction of phosphorylated NF-κB by LPS stimulation was not observed in THP-1 cells treated with tunicamycin. (B) Fluorescence microscopy examination of the tunicamycin-treated THP-1 cells followed by LPS stimulation. Cells were permeabilized and were stained with anti- NF-κB p65 and tetramethyl rhodamine isothiocyanate-goat anti-mouse IgG (red). The nucleus is stained with DAPI (4, 6-diamino-2-phenylindole; blue). The sustained localization of NF-κB p65 in the cytoplasm was observed in THP-1 cells treated with tunicamycin followed by LPS stimulation. Original magnification, ×400. Filled bars; no treatment. Open bar; treatment with tunicamycin (5 μg/ml). $^{*}P < 0.01$.

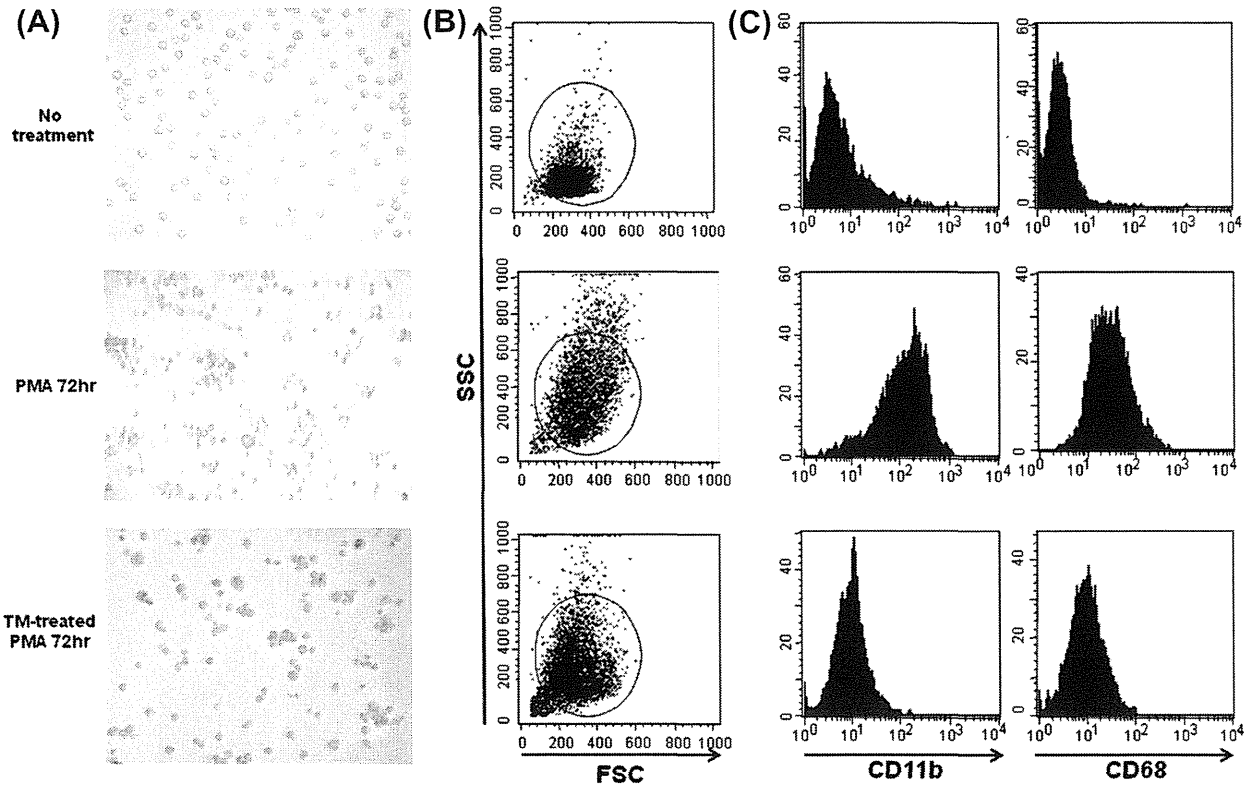

Fig. 5. Human monocytes under ER stress demonstrated impaired capability for differentiation into macrophages. (A–E) Conditioning with tunicamycin (5 μg/ml) THP-1 cells were treated with PMA (50 ng/ml) for 72 h. Cells were examined under microscopy for morphology and flow cytometry for surface molecules of macrophage markers CD11b and CD68. Gene expression of cells was also analyzed by RTD-PCR for CD11b, CD68, CHOP and BiP. Morphological analysis (A) and scatter and forward scatter by flow cytometry (B) PMA-differentiated THP-1 cells conditioned with tunicamycin were observed to be smaller and less granular compared to cells not treated with tunicamycin. Flow cytometry analysis (C) and gene expression analysis by RTD-PCR (D) for markers of macrophages, CD11b and CD68 showed decreased expression of these markers in THP-1 cells treated with tunicamycin and PMA. (E) Gene expressions of CHOP and BiP were increased in THP-1 cells conditioned with tunicamycin. (F–H) Primary human monocytes treated with tunicamycin (0.1 μg/ml) were cultured with GM-CSF (100 ng/ml) for 4 days for differentiation into macrophages. Cultured cells were examined by microscopy and flow cytometry. Tunicamycin-treated primary human monocytes were smaller (F) and less granular (G), and CD11b expression was repressed (H) after 4 days culture in media with GM-CSF. Data are expressed as means ± SEM of four independent experiments. Filled bars; no treatment. Open bar; treatment with tunicamycin (5 μg/ml). $^{**}P < 0.01$, $^{***}P < 0.001$.

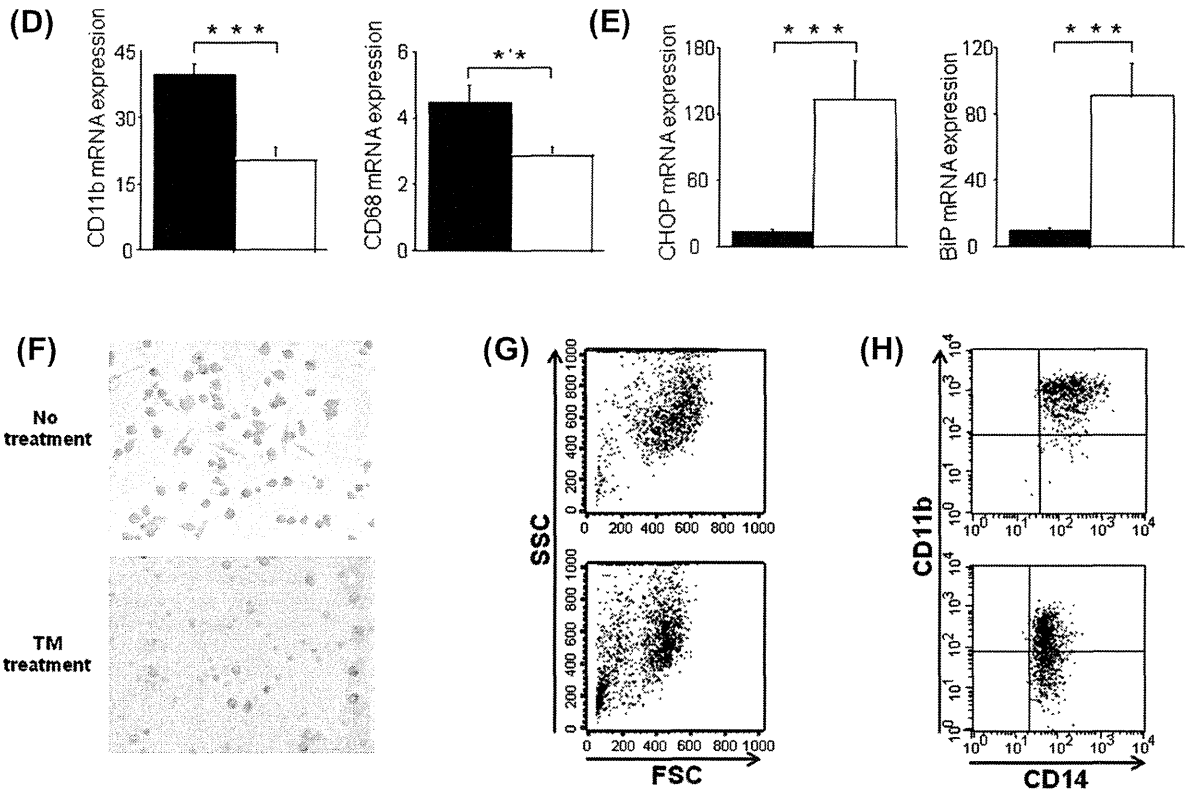

Fig. 5. (*continued*)

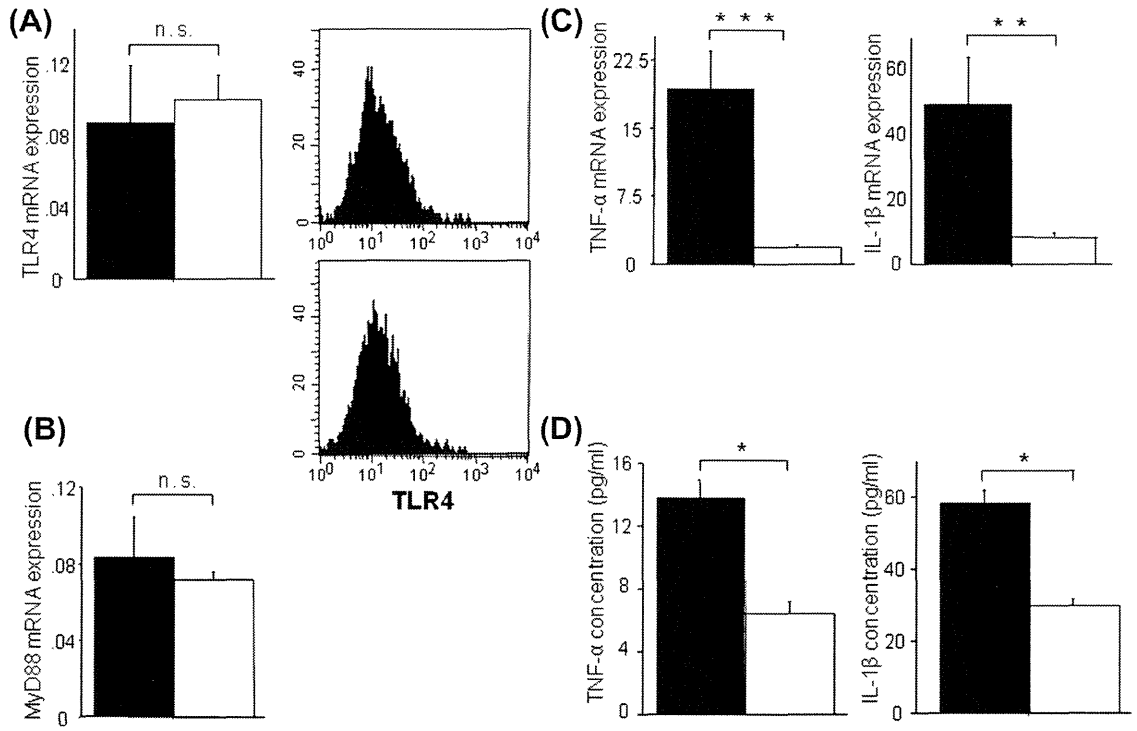

Fig. 6. The expression of proinflammatory cytokines in response to LPS stimulation was decreased in PMA-driven differentiated macrophage-like cells under ER stress without alteration of the expression of TLR4 and accessory molecules. THP-1 cells were treated with tunicamycin (5 μg/ml) followed by PMA treatment for differentiation induction into macrophages. Expression analysis by RTD-PCR (A) and flow cytometry (B) was performed for TLR4 and MyD88. Expressions of both molecules were not affected. (C–D) THP-1 cells were treated with tunicamycin (5 μg/ml) followed by PMA treatment for 72 h followed by LPS stimulation. Gene expression analysis (C) of cells stimulated with LPS for 3 h as well as ELISA quantification (D) of concentrations of cells stimulated with LPS for 12 h in culture medium were assessed. The expressions of TNF-α and IL-1β in response to LPS stimulation were significantly decreased in differentiated macrophage-like cells when they were under ER stress by tunicamycin. Filled bars; no treatment. Open bar; treatment with tunicamycin (5 μg/ml).

4. Discussion

We observed that ER stress induced susceptibility to apoptosis in THP-1 cells, a human monocytic cell line. Functionally, the response of LPS-stimulated human monocytes to express proinflammatory cytokines under ER stress was attenuated prior to the obvious appearance of apoptosis, with decreased activation of NF-κB. Furthermore, the differentiation capability of monocytes into macrophages was inhibited with a hypo-responsiveness to LPS under ER stress. These observations suggest that ER stress is an important pathological condition affecting a variety of monocyte functions.

The ER system is indispensable for synthesizing properly functioning proteins [1]. Under ER stress, cells malfunction due to the improper production or folding of proteins. Therefore, ER stress can result in the retention of harmful unfolded proteins as a consequence of impaired function of ER-related molecules such as protein kinase R-like ER kinase (PERK), inositol requiring enzyme 1 (IRE1), and activating transcription factor 6 (ATF6), all of which are important molecules of the ER system [17,18]. In the immune system, an unfolded protein response (UPR) related to ER stress was observed in myeloma cells, malignant cells of plasma cells [19]. The affected immune response due to an UPR was also observed in the development of nonmalignant immunological disorders, such as rheumatoid arthritis and neurodegenerative disease [2]. UPRs affect the survival and function of DCs because of their pivotal capacity to process peptides for presentation and secrete cytokines [20]. These findings, as well as our previous observation that diabetic monocytes were under ER stress and were impaired [11], demonstrate that monocytes are an important subpopulation in immune cells in ER stress-related diseases.

Prolonged ER stress leads to apoptotic cell death, which is mediated by CHOP [21], a crucial specific molecule for ER stress-induced apoptosis. Apoptosis is also accompanied by alterations of the transcriptional expression of the BCL-2 gene family [22]. We observed that THP-1 monocytic cells under ER stress underwent apoptosis with decreased expression of the anti-apoptotic molecule BCL-2, indicating that ER stress induced THP-1 cell death using conventional apoptotic pathways [23,24].

The TLR pattern recognition by the innate immune system induces proinflammatory cytokines through the activation of NF-κB [25,26]. In the quiescent state, NF-κB remains inactive in the cytoplasm through binding to the inhibitory protein IκB. The phosphorylated IκB releases NF-κB to translocate into the nucleus where it mediates the transcription of its target genes [14]. We observed that the tunicamycin-induced ER stress diminished TLR4 signaling without altering the expressions of TLR4 and MyD88. With regard to the transcriptional factor, we observed a lack of the activated form of NF-κB and sustained cytoplasmic localization of NF-κB in LPS-stimulated THP-cells under ER stress. The activation of NF-κB is transient and cyclic upon continuous stimulation, which is due to specific negative feedback control systems such as the NF-κB inducible synthesis of IκB and A20 [27]. A previous report indicated that ER stress-induced A20, a deubiquitinating protease [28], acts as an inhibitor of NF-κB [29,30]. We observed that ER stress by tunicamycin treatment induced the expression of BiP, an important chaperone involved in quality control. BiP was previously reported to decrease the activation of NF-κB [31], and is a potent extracellular anti-inflammatory molecule [32]. Thus, these molecules may be related to the underlining mechanism of the attenuated TLR4 signaling by ER stress involving decreased activation of NF-κB. Although some molecules related to ER stress, such as A20 and BiP, were previously reported to be involved in decreased NF-κB activation, we were unable to identify a specific mechanistic ER stress pathway directly related to impaired TLR4-induced expression of TNF-α and IL-1β. Impaired TLR signaling in the presence of tunicamycin was not observed following treatment with specific inhibitors of IRE-1, ATF6, or PERK (data not shown), suggesting that multiple pathways regulate this effect. Further investigation of how ER stress-related molecules are involved in inhibition of NF-κB under ER stress in terms of cellular machinery is, therefore, warranted.

Diabetes is associated with chronic inflammation [33,34]. Although smoldering inflammation is a fundamental pathological condition of diabetic patients, a characteristic of their immunity is the hypo-responsiveness to pathogenic stimulation [35]. We observed that NF-κB was, to some extent, activated in THP-1 cells under ER stress induced by tunicamycin before TLR4 ligand stimulation, despite the attenuated signal transduction to TLR ligand stimulation in monocytes (Fig. 4A). ER stress slightly increased the activated form of NF-κB in the quiescent condition before external ligand stimulation. This finding may correspond to the smoldering inflammation of diabetes, whereas the hypo-responsiveness to impaired TLR4 signaling under ER stress is consistent with the impaired immunity of diabetes. Further investigations are needed to elucidate the details of the chronic inflammation status and the systemic immunity condition.

Monocytes are progenitor cells that can differentiate into mature resident macrophages in various human tissues and become important immune regulators that control the acquired immune response [36]. Monocyte differentiation to macrophages is characterized as a reduction in the nucleocytoplasmic ratio [37] and enhanced granularity [38], which was observed in THP-1 cells (Fig. 5A) and primary human monocytes (Fig. 5C). The morphological maturity of macrophage differentiation was not observed in cells under tunicamycin-induced ER stress. Furthermore, the characteristic change of surface markers in the monocyte/macrophage lineage was also affected, showing decreased expressions of macrophage differentiation markers. A previous report suggested that the inhibition of NF-κB activation is involved in the impairment of monocyte differentiation into macrophages in THP-1 cells [39]. Therefore, the affected NF-κB activation and subcellular localization under ER stress may explain, in part, the affected differentiation capability of monocytes into macrophages.

We observed that TLR4 signaling was impaired in differentiated macrophages when they were under tunicamycin-induced ER stress (Fig. 6). Therefore, ER stress may broadly affect the monocytic lineage cells that express the pattern recognition molecules related to innate immunity, implying that ER stress is also a significant condition that broadly impairs host immunity.

In conclusion, our findings demonstrate that ER stress affects the pathogenic ligand-induced TLR signaling as a consequence of attenuated activation of NF-κB, as well as the differentiation capability into macrophages, which are the important functional regulators of the immune reaction. Further investigations are needed to elucidate the mechanisms of ER stress-related perturbations of the immune reaction in association with various diseases.

Conflict of interest

The authors declare no competing financial interests.

Appendix A. Supplementary data

Supplementary data associated with this article can be found, in the online version, at http://dx.doi.org/10.1016/j.cellimm.2013.04.006.

References

[1] B. Kleizen, I. Braakman, Protein folding and quality control in the endoplasmic reticulum, Curr. Opin. Cell Biol. 16 (2004) 343–349.

[2] M. Aridor, W.E. Balch, Integration of endoplasmic reticulum signaling in health and disease, Nat. Med. 5 (1999) 745–751.
[3] C. Xu, B. Bailly-Maitre, J.C. Reed, Endoplasmic reticulum stress: cell life and death decisions, J. Clin. Invest. 115 (2005) 2656–2664.
[4] Y. Ma, L.M. Hendershot, The role of the unfolded protein response in tumor development: friend or foe?, Nat Rev. Cancer 4 (2004) 966–977.
[5] U. Ozcan, Q. Cao, E. Yilmaz, A.H. Lee, N.N. Iwakoshi, E. Ozdelen, G. Tuncman, C. Görgün, L.H. Glimcher, G.S. Hotamisligil, Endoplasmic reticulum stress links obesity, insulin action, and type 2 diabetes, Science 306 (2004) 457–461.
[6] G.K. Hansson, Inflammation, atherosclerosis, and coronary artery disease, N. Engl. J. Med. 352 (2005) 1685–1695.
[7] J.P. Taylor, J. Hardy, K.H. Fischbeck, Toxic proteins in neurodegenerative disease, Science 296 (2002) 1991–1995.
[8] S. Akira, S. Uematsu, O. Takeuchi, Pathogen recognition and innate immunity, Cell 124 (2006) 783–801.
[9] C. Pasare, R. Medzhitov, Toll-like receptors: linking innate and adaptive immunity, Microbes. Infect. 6 (2004) 1382–1387.
[10] S. Gordon, P.R. Taylor, Monocytes and macrophage heterogeneity, Nat. Rev. Immunol. 5 (2005) 953–964.
[11] T. Komura, Y. Sakai, M. Honda, T. Takamura, K. Matsushima, S. Kaneko, CD14$^+$ monocytes are vulnerable and functionally impaired under ER stress in patients with type 2 diabetes, Diabetes 59 (2010) 634–643.
[12] M. Tateno, M. Honda, T. Kawamura, H. Honda, S. Kaneko, Expression profiling of peripheral-blood mononuclear cells from patients with chronic hepatitis C undergoing interferon therapy, J. Infect. Dis. 195 (2007) 255–267.
[13] S. Thoma-Uszynski, S. Stenger, O. Takeuchi, M.T. Ochoa, M. Engele, P.A. Sieling, P.F. Barnes, M. Rollinghoff, P.L. Bolcskei, M. Wagner, S. Akira, M.V. Norgard, J.T. Belisle, P.J. Godowski, B.R. Bloom, R.L. Modlin, Induction of direct antimicrobial activity through mammalian toll-like receptors, Science 291 (2001) 1544–1547.
[14] M.S. Hayden, S. Ghosh, Shared principles in NF-kappaB signaling, Cell 132 (2008) 344–362.
[15] F. Wong, C. Hull, R. Zhande, J. Law, A. Karsan, Lipopolysaccharide initiates a TRAF6-mediated endothelial survival signal, Blood 103 (2004) 4520–4526.
[16] N.V. Serbina, T. Jia, T.M. Hohl, E.G. Pamer, Monocyte-mediated defense against microbial pathogens, Annu. Rev. Immunol. 26 (2008) 421–452.
[17] D. Ron, P. Walter, Signal integration in the endoplasmic reticulum unfolded protein response, Nat. Rev. Mol. Cell Biol. 8 (2007) 519–529.
[18] B. Bukau, J. Weisseman, A. Horwich, Molecular chaperones and protein quality control, Cell 125 (2006) 443–451.
[19] D.T. Rutkowski, R.J. Kaufman, A trip to the ER: coping with stress, Trends Cell Biol. 14 (2004) 20–28.
[20] N.N. Iwakoshi, M. Pypaert, L.H. Glimcher, The transcription factor XBP-1 is essential for the development and survival of dendritic cells, J. Exp. Med. 204 (2007) 2267–2275.
[21] X.Z. Wang, D. Ron, Stress-induced phosphorylation and activation of the transcription factor CHOP (GADD153) by p38 MAP kinase, Science 272 (1996) 1347–1349.
[22] K.D. McCullough, J.L. Martindale, L.O. Klotz, T.Y. Aw, N.J. Holbrook, Gadd153 sensitizes cells to endplasmic reticulum stress by down-regulating Bcl2 and perturbing the cellular redox state, Mol. Cell. Biol. 21 (2001) 1249–1259.
[23] T. Gotoh, K. Terada, S. Oyadomari, M. Mori, Hsp70-DnaJ chaperone pair prevents nitric oxide- and CHOP-induced apoptosis by inhibiting translocation of Bax to mitochondria, Cell Death Differ. 11 (2004) 390–402.
[24] I. Tabas, D. Ron, Integrating the mechanisms of apoptosis induced by endoplasmic reticulum stress, Nat. Cell Biol. 13 (2011) 184–190.
[25] A. Iwasaki, R. Medzhitov, Toll-like receptor control of the adaptive immune responses, Nat. Immunol. 10 (2004) 987–995.
[26] I. Sabroe, L.C. Parker, S.K. Dower, M.K. Whyte, The role of TLR activation in inflammation, J. Pathol. 214 (2008) 126–135.
[27] S.L. Werner, J.D. Kearns, V. Zadorozhnaya, C. Lynch, C. OLynch, M.P. Boldin, A. Ma, D. Baltimore, A. Hoffmann, Encoding NF-kappaB temporal control in response to TNF: distinct roles for the negative regulators IkappaBalpha and A20, Gene Dev. 22 (2008) 2093–2101.
[28] K. Hayakawa, N. Hiramatsu, M. Okamura, H. Yamazaki, S. Nakajima, J. Yao, A.W. Paton, J.C. Paton, M. Kitamura, Acquisition of anergy to proinflammatory cytokines in nonimmune cells through endoplasmic reticulum stress response: a mechanism for subsidence of inflammation, J. Immunol. 182 (2009) 1182–1191.
[29] K. Heyninck, R. Beyaert, A20 inhibits NF-κB activation by dual ubiquitin-editing functions, Trends Biochem. Sci. 30 (2005) 1–4.
[30] A. Krikos, C.D. Laherty, V.M. Dixit, Transcriptional activation of the tumor necrosis factor alpha-inducible zinc finger protein, A20, is mediated by kappa B elements, J. Biol. Chem. 267 (1992) 17971–17976.
[31] S. Nakajima, N. Hiramatsu, K. Hayakawa, Y. Saito, H. Kato, T. Huang, J. Yao, A.W. Paton, J.C. Paton, M. Kitamura, Selective Abrogation of BiP/GRP78 Blunts Activation of NF-κB through the ATF6 Branch of the UPR: Involvement of C/EBP and mTOR-Dependent Dephosphorylation of Akt, Mol. Cell. Biol. 31 (2011) 1710–1718.
[32] V.M. Corrigall, M.D. Bodman-Smith, M. Brunst, H. Cornell, G.S. Panayi, Inhibition of Antigen-Presenting Cell Function and Stimulation of Human Peripheral Blood Mononuclear Cells to Express an Antiinflammatory Cytokine Profile by the Stress Protein BiP, Arthritis. Rheum. 50 (2004) 1164–1171.
[33] K.E. Wellen, G.S. Hotamisligil, Inflammation, stress and diabetes, J. Clin. Invest. 115 (2005) 1111–1119.
[34] M. Stumvoll, B.J. Goldstein, T.W. van Haeften, Type 2 diabetes: principles of pathogenesis and therapy, Lancet 365 (2005) 1333–1346.
[35] C.P. Liang, S. Han, T. Senokuchi, A.R. Tall, The macrophage at the crossroads of insulin resistance and atherosclerosis, Circ. Res. 100 (2007) 1546–1555.
[36] G. Siamon, R.T. Philip, Monocyte and macrophage heterogeneity, Nat. Rev. Immunol. 5 (2005) 953–964.
[37] R.J. Sokol, G. Hudson, N.T. James, I.J. Frost, J. Wales, Human macrophage development: a morphometric study, J. Anat. 151 (1987) 27–35.
[38] K.C. McCullough, S. Basta, S. Knötig, H. Gerber, R. Schaffner, Y.B. Kim, A. Saalmüller, A. Summerfield, Intermediate stages in monocyte-macrophage differentiation modulate phenotype and susceptibility to virus infection, Immunology 98 (1999) 203–212.
[39] Y.S. Chuang, S.H. Yang, T.Y. Chen, J.H. Pang, Cilostazol inhibits matrix invasion and modulates the gene expressions of MMP-9 and TIMP-1 in PMA-differentiated THP-1 cells, Eur. J. Pharmacol. 670 (2011) 419–426.

JVI Journals.ASM.org

MicroRNA-27a Regulates Lipid Metabolism and Inhibits Hepatitis C Virus Replication in Human Hepatoma Cells

Takayoshi Shirasaki,[a,b] Masao Honda,[a,b] Tetsuro Shimakami,[a] Rika Horii,[a] Taro Yamashita,[a] Yoshio Sakai,[a] Akito Sakai,[a] Hikari Okada,[a] Risa Watanabe,[b] Seishi Murakami,[a] MinKyung Yi,[c] Stanley M. Lemon,[d] Shuichi Kaneko[a]

Department of Gastroenterology, Kanazawa University Graduate School of Medical Science, Kanazawa, Japan[a]; Department of Advanced Medical Technology, Kanazawa University Graduate School of Health Medicine, Kanazawa, Japan[b]; Human Center for Hepatitis Research, Institute for Human Infections and Immunity, and Department of Microbiology and Immunology, University of Texas Medical Branch, Galveston, Texas, USA[c]; Division of Infectious Diseases, School of Medicine, The University of North Carolina at Chapel Hill, Chapel Hill, North Carolina, USA[d]

The replication and infectivity of the lipotropic hepatitis C virus (HCV) are regulated by cellular lipid status. Among differentially expressed microRNAs (miRNAs), we found that miR-27a was preferentially expressed in HCV-infected liver over hepatitis B virus (HBV)-infected liver. Gene expression profiling of Huh-7.5 cells showed that miR-27a regulates lipid metabolism by targeting the lipid synthetic transcription factor RXRα and the lipid transporter ATP-binding cassette subfamily A member 1. In addition, miR-27a repressed the expression of many lipid metabolism-related genes, including *FASN*, *SREBP1*, *SREBP2*, *PPARα*, and *PPARγ*, as well as *ApoA1*, *ApoB100*, and *ApoE3*, which are essential for the production of infectious viral particles. miR-27a repression increased the cellular lipid content, decreased the buoyant density of HCV particles from 1.13 to 1.08 g/cm^3, and increased viral replication and infectivity. miR-27a overexpression substantially decreased viral infectivity. Furthermore, miR-27a enhanced *in vitro* interferon (IFN) signaling, and patients who expressed high levels of miR-27a in the liver showed a more favorable response to pegylated IFN and ribavirin combination therapy. Interestingly, the expression of miR-27a was upregulated by HCV infection and lipid overload through the adipocyte differentiation transcription factor C/EBPα. In turn, upregulated miR-27a repressed HCV infection and lipid storage in cells. Thus, this negative feedback mechanism might contribute to the maintenance of a low viral load and would be beneficial to the virus by allowing it to escape host immune surveillance and establish a persistent chronic HCV infection.

MicroRNA (miRNA) is a small, endogenous, single-stranded, noncoding RNA consisting of 20 to 25 bases that regulates gene expression. It plays an important role in various biological processes, including organ development, differentiation, and cellular death and proliferation, and is also involved in infection and diseases such as cancer (1).

Previously, we examined miRNA expression in hepatocellular carcinoma (HCC) and noncancerous background liver tissue infected with hepatitis B virus (HBV) and HCV (2). We showed that some miRNAs were differentially expressed according to HBV or HCV infection but not according to the presence of HCC. These infection-specific miRNAs were believed to regulate HBV or HCV replication; however, their functional role has not been elucidated.

HCV is described as a lipotropic virus because of its association with serum lipoprotein (3–5). It utilizes the low-density lipoprotein (LDL) receptor for cellular entry (6–8) and forms replication complexes on lipid rafts (9). The HCV core protein surrounds and binds lipid droplets (LDs) and nonstructural proteins on the endoplasmic reticulum (ER) membrane, which is essential for particle formation (10). Moreover, HCV cellular secretion is linked to very LDL (VLDL) secretion (11). In liver tissue histology, steatosis is often observed in chronic hepatitis C (CH-C) and is closely related to resistance to interferon (IFN) treatment (12, 13). Thus, lipids play important roles in HCV replication and CH-C pathogenesis.

Several miRNAs, such as miR-122 (14), miR-199a (15), miR-196 (16), miR-29 (17), Let-7b (18), and miR-130a (19), reportedly regulate HCV replication; however, miRNAs that regulate lipid metabolism and HCV replication have not been reported so far. Previously, we reported that 19 miRNAs were differentially expressed in HBV- and HCV-infected livers (2). In the present study, we evaluated the functional relevance of miR-27a in HCV replication by using the human hepatoma cell line Huh-7.5. We analyzed the regulation of lipid metabolism by miR-27a in hepatocytes and revealed a unique pathophysiological relationship between lipid metabolism and HCV replication in CH-C.

MATERIALS AND METHODS

Cell line. Huh-7.5 cells (kindly provided by C. M. Rice, Rockefeller University, New York, NY) were maintained in Dulbecco's modified Eagle's medium (DMEM; Gibco BRL, Gaithersburg, MD) containing 10% fetal bovine serum (FBS) and 1% penicillin-streptomycin.

HCV replication analysis. HCV replication analysis was performed by transfecting Huh-7.5 cells with JFH-1 (20), H77Sv2 Gluc2A (21), and their derivative RNA constructs. pH77Sv2 is a modification of pH77S, a plasmid containing the full-length sequence of the genotype 1a H77 HCV strain with five cell culture-adaptive mutations that promote its replication in Huh-7 hepatoma cells (21–24). pH77Sv2 Gluc2A is a related construct in which the *Gaussia* luciferase (Gluc) sequence, fused to the 2A autocatalytic protease of foot-and-mouth virus RNA, was inserted in frame between p7 and NS2 (21, 23, 25). pH77Sv2 Gluc2A (AAG) is a control plasmid that has an NS5B polymerase catalytic domain mutation.

Received 29 October 2012 Accepted 21 February 2013
Published ahead of print 28 February 2013
Address correspondence to Masao Honda, mhonda@m-kanazawa.jp.

doi:10.1128/JVI.03022-12

For RNA transfection, the cells were washed with phosphate-buffered saline (PBS) and resuspended in complete growth medium. The cells were then pelleted by centrifugation (1,400 × *g* for 4 min at 4°C), washed twice with ice-cold PBS, and resuspended in ice-cold PBS at a concentration of 7.5×10^6 cells/0.4 ml. The cells were mixed with 10 μg of the RNA transcripts, placed into 2-mm-gap electroporation cuvettes (BTX Genetronics, San Diego, CA), and electroporated with five pulses of 99 μs at 750 V over 1.1 s in an ECM 830 (BTX Genetronics). Following a 10-min recovery period, the cells were mixed with complete growth medium and plated.

miR-27a and anti-miR-27a transfection. Huh-7.5 cells transfected with pH77Sv2 Gluc2A RNA or pH77Sv2 Gluc2A (AAG) RNA were transfected with 50 nM synthetic miRNA (pre-miRNA) or 50 nM anti-miRNA (Ambion Inc., Austin, TX) with the siPORTTM NeoFXTM Transfection Agent (Ambion). Transfection was performed immediately by mixing the electroporated cells with the miRNA transfection reagents. Control samples were transfected with an equal concentration of a nontargeting control (pre-miRNA negative control) or inhibitor negative control (anti-miRNA negative control) to assess non-sequence-specific effects in the miRNA experiments.

Fatty acid treatment. Huh-7.5 cells transfected with HCV RNA and pre- or anti-miRNA were cultured for 24 h and then treated with the indicated concentrations of oleic acid (0 to 250 μM) (26) in the presence of 2% free fatty acid (FFA)-free bovine serum albumin (BSA; Sigma-Aldrich, St. Louis, MO). The cells were harvested at 72 h posttreatment with oleic acid for quantitative real-time detection PCR (RTD-PCR), Western blotting, immunofluorescence staining, and reporter analysis. The number of viable cells was determined by an MTS assay [one-step 3-(4,5-dimethylthiazol-2-yl)-2,5-diphenyltetrazolium bromide assay; Promega Corporation, Madison, WI]. Cellular triglyceride (TG) and cholesterol (TCHO) contents were measured with TG Test Wako and Cholesterol Test Wako kits (Wako, Osaka, Japan) according to the manufacturer's instructions.

Equilibrium ultracentrifugation of JFH-1 particles in isopycnic iodixanol gradients. Filtered supernatant fluids collected from JFH-1 RNA- and pre-miRNA- or anti-miRNA-transfected cell cultures were concentrated 30-fold with a Centricon PBHK Centrifugal Plus-20 filter unit with an Ultracel PL membrane (100-kDa exclusion; Merck Millipore, Billerica, MA) and then layered on top of a preformed continuous 10 to 40% iodixanol (OptiPrep; Sigma-Aldrich) gradient in Hanks' balanced salt solution (Invitrogen, Carlsbad, CA) as described previously (24). The gradients were centrifuged in an SW41 rotor (Beckman Coulter Inc., Brea, CA) at 35,000 rpm for 16 h at 4°C, and the fractions (500 μl each) were collected from the top of the tube. The density of each fraction was determined with a digital refractometer (Atago, Tokyo, Japan).

Infectivity assays. Huh-7.5 cells were seeded at 5.0×10^4/well in 48-well plates 24 h before inoculation with 100 μl of the gradient fractions. The cells were tested for the presence of intracellular core antigen by immunofluorescence 72 h later, as described below. Clusters of infected cells that stained for the core antigen were considered to constitute a single infectious focus, and virus titers were calculated accordingly in terms of numbers of focus-forming units (FFU)/ml.

Western blotting and immunofluorescence staining. Western blotting was performed as described previously (27). The cells were washed in PBS and lysed in radioimmunoprecipitation assay buffer containing Complete protease inhibitor cocktail and PhosSTOP (Roche Applied Science, Indianapolis, IN). The membranes were blocked in Blocking One or Blocking One-P solution (Nacalai Tesque, Kyoto, Japan), and the expression of HCV core protein, retinoid X receptor alpha (RXRα), sterol regulatory element-binding protein (SREBP1), ATP-binding cassette subfamily A member 1 (ABCA1), ApoE3, ApoB100, fatty acid synthase (FASN), peroxisome proliferator-activated receptor α (PPARα), ApoA1, phospho-PKR-like ER kinase (phospho-PERK), PERK, phospho-eIF2α, eIF2α, BIP, phospho-STAT1, and β-actin was evaluated with mouse anti-core (Thermo Fisher Scientific Inc., Rockford, IL), rabbit anti-RXRα, rabbit anti-SREBP1 (Santa Cruz Biotechnology Inc., Santa Cruz, CA), mouse anti-ABCA1 (Abcam, Cambridge, MA), goat anti-ApoE3, goat anti-ApoB100 (R&D Systems Inc., Minneapolis, MN), rabbit anti-FASN, rabbit anti-PPARα, mouse anti-ApoA1, rabbit anti-phospho-PERK, rabbit anti-PERK, rabbit anti-phospho-eIF2α, rabbit anti-eIF2α, rabbit anti-BIP, rabbit anti-phospho-STAT1, and rabbit anti-β-actin antibodies (Cell Signaling Technology Inc., Danvers, MA), respectively.

For immunofluorescence staining, the cells were washed twice with PBS and fixed in 4% paraformaldehyde for 15 min at room temperature. After washing again with PBS, the cells were permeabilized with 0.05% Triton X-100 in PBS for 15 min at room temperature. They were then incubated in a blocking solution (10% FBS and 5% BSA in PBS) for 30 min and with the anti-core monoclonal antibodies. The fluorescent secondary antibodies were Alexa 568-conjugated anti-mouse IgG antibodies (Invitrogen). Nuclei were labeled with 4′,6-diamidino-2-phenylindole (DAPI), and LDs were visualized with boron-dipyrromethene (BODIPY) 493/503 (Invitrogen). Imaging was performed with a CSU-X1 confocal microscope (Yokogawa Electric Corporation, Tokyo, Japan).

Quantitative RTD-PCR. Total RNA was isolated with a GenElute Mammalian Total RNA Miniprep kit (Sigma-Aldrich), and cDNA was synthesized with a high-capacity cDNA reverse transcription kit (Applied Biosystems, Carlsbad, CA). The primer pairs and probes for C/EBPα, ABCA1, PPARγ, SREBF1, SREBF2, FASN, 2′-5′-oligoadenylate synthetase 2 (OAS2), and β-actin were obtained from the TaqMan assay reagent library. HCV RNA was detected as described previously (28). HCV RNA was isolated from viral particles with a QIAamp viral RNA kit (Qiagen, Inc., Valencia, CA) in accordance with the manufacturer's instructions. Total RNA containing miRNA was isolated according to the protocol of the mirVana miRNA isolation kit (Ambion). For the enrichment of mature miRNA, argonaute 2 (Ago2)-binding miRNA was immunoprecipitated with an anti-Ago2 monoclonal antibody (Wako) and mature miRNA was eluted from the precipitant with a microRNA isolation kit, Human Ago2 (Wako). cDNA was prepared via reverse transcription with 10 ng of isolated total RNA and 3 μl of each reverse transcription primer with specific loop structures. Reverse transcription was performed with a TaqMan MicroRNA reverse transcription kit (Applied Biosystems) according to the manufacturer's protocol. RTD-PCR was performed with the 7500 Real Time PCR system (Applied Biosystems) according to the manufacturer's instructions. The primer pairs and probes for miR-let7a, miR-34c, miR-142-5p, miR-27a, miR-23a, and RNU6B were obtained from the TaqMan assay reagent library.

3′ UTR luciferase reporter assays. The miRNA expression reporter vector pmirGLO Dual-Luciferase miRNA Target Expression Vector (Promega Corporation) was used to validate the RXRα and ABCA1 3′ untranslated regions (UTRs) as miRNA binding sites. cDNA fragments corresponding to the entire 3′ UTR of human RXRα and human ABCA1 were amplified with the Access RT-PCR system (Promega Corporation) from total RNA extracted from Huh-7.5 cells. The PCR products were cloned into the designated multiple cloning site downstream of the luciferase open reading frame between the SacI and XhoI restriction sites of the pCR2.1-TOPO vector (Invitrogen). Point mutations in the seed region of the predicted miR-27a sites within the 3′ UTR of human RXRα and human ABCA1 were generated with a QuikChange Multi site-directed mutagenesis kit (Agilent Technologies Inc., Santa Clara, CA) according to the manufacturer's protocol. All constructs were confirmed by sequencing.

Huh-7.5 cells were grown to 70% confluence in 24-well plates in complete DMEM. The cells were cotransfected with 200 ng of the indicated 3′ UTR luciferase reporter vector and 50 nM synthetic miRNA (pre-miRNA) or 50 nM anti-miRNA (Ambion) in a final volume of 0.5 ml with Lipofectamine 2000 (Invitrogen). At 24 h posttransfection, firefly and *Renilla* luciferase activities were measured consecutively with the Dual-Luciferase Reporter Assay system (Promega Corporation).

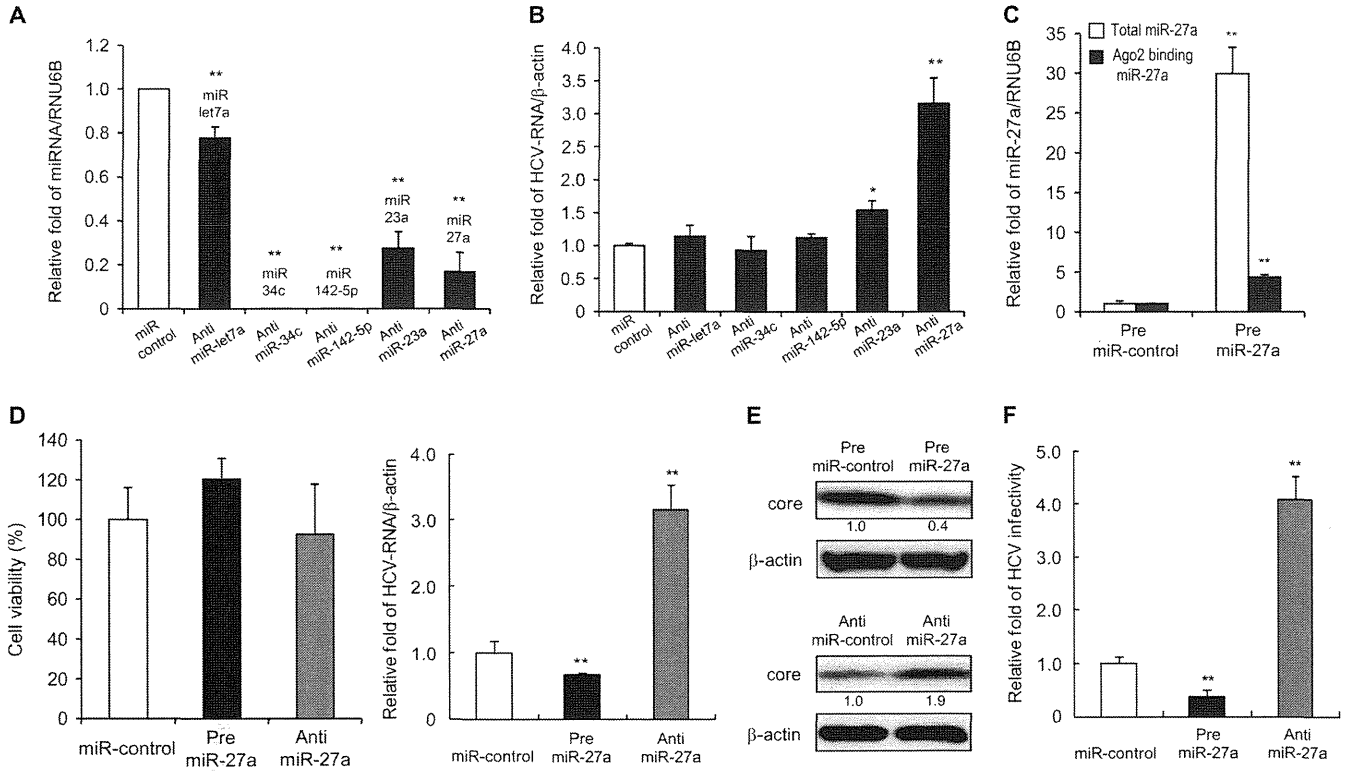

FIG 1 miR-27a has a negative effect on HCV replication and infectivity. Huh-7.5 cells were transfected with JFH-1 RNA and pre- or anti-miRNA. Expression was quantified at 72 h posttransfection. (A) Inhibition efficiency of miRNAs by anti-miRNAs (RTD-PCR, $n = 6$). (B) Effects of anti-miRNAs on HCV replication (RTD-PCR, $n = 6$). (C) Detection of whole miR-27a and Ago2-binding miR-27a in Huh-7.5 cells. At 72 h posttransfection, cells were harvested and Ago2-binding miRNA was purified as described in Materials and Methods. White bars indicate total miR-27a levels, and black bars indicate Ago2-binding miR-27a levels (RTD-PCR, $n = 6$). (D) Effects of pre- or anti-miR-27a on cell viability (left) and HCV replication (right). Cell viability (%) was assessed by the MTS assay ($n = 6$). (E) Effects of pre- or anti-miR-27a on HCV core protein levels by Western blotting. (F) Effects of pre- or anti-miR-27a on HCV infection. Huh-7.5 cells were infected with HCVcc derived from Huh-7.5 cells transfected with pre- or anti-miR-27a and JFH-1 RNA. HCV RNA was quantified at 72 h postinfection by RTD-PCR ($n = 6$). All experiments were performed in duplicate and repeated three times. Values are means ± standard errors. *, $P < 0.01$; **, $P < 0.005$.

Promoter analysis. DNA fragments from −400 to +36 bp and from −700 to +36 bp relative to the transcription initiation site of pri-miR-23a~27a~24-2 were inserted into pGL3-Basic (Promega Corporation) at the MluI and XhoI sites. Point mutations in the seed region of predicted C/EBPα binding sites were generated with a QuikChange Multi site-directed mutagenesis kit (Agilent Technologies) according to the manufacturer's protocol. All constructs were confirmed by sequencing.

Huh-7.5 cells transfected with HCV RNA were cultured for 24 h in 24-well plates, and then 200 ng of the plasmids was cotransfected with 2 ng of the *Renilla* luciferase expression vector (pSV40-Renilla) with the FuGENE6 Transfection Reagent (Roche Applied Science). After 24 h, the cells were treated with oleic acid in the presence of 2% FFA-free BSA (Sigma-Aldrich). At 48 h posttreatment, a luciferase assay was carried out with the Dual-Luciferase Reporter Assay system (Promega Corporation) according to the manufacturer's instructions.

For tunicamycin treatment, the plasmids (200 ng) were cotransfected with 2 ng pSV40-Renilla with FuGENE6 (Roche Applied Science) into Huh-7.5 cells grown in the wells of 24-well plates. After 24 h, the cells were treated for a further 24 h with the indicated concentrations of tunicamycin and a luciferase assay was carried out as described above.

RNA interference. A small interfering RNA (siRNA) specific to ABCA1 and a control siRNA were obtained from Thermo Fisher Scientific. Transfection was performed with Lipofectamine 2000 (Invitrogen) according to the manufacturer's instructions.

IFN treatment. Huh-7.5 cells transfected with HCV RNA and pre- or anti-miRNA were treated with oleic acid as described above. At 48 h later, the cells were treated with the indicated number of international units of IFN-α for 24 h.

Affymetrix GeneChip analysis. Aliquots of total RNA (50 ng) isolated from the cells were subjected to amplification with the WT-Ovation Pico RNA Amplification system (NuGen, San Carlos, CA) according to the manufacturer's instructions. The Affymetrix Human U133 Plus 2.0 microarray chip containing 54,675 probes has been described previously (29).

Statistical analysis. Results are expressed as mean values ± standard errors. At least six samples were tested in each assay. Significance was tested by one-way analysis of variance with Bonferroni methods, and differences were considered statistically significant at P values of <0.01 (*, $P < 0.01$; **, $P < 0.005$).

Microarray accession number. The expression data determined in this study were deposited in the Gene Expression Omnibus database (NCBI) under accession number GSE41737.

RESULTS

Functional relevance of the upregulated miRNAs in HCV-infected livers. Previously, 19 miRNAs were shown to be differentially expressed in HBV- and HCV-infected livers (2). Of these, 6 miRNAs were upregulated and 13 were downregulated. In this study, we focused on the upregulated miRNAs, as they might play a positive role in HCV replication. Anti-miRNAs and the control miRNA were transfected into Huh-7.5 cells following JFH-1 RNA

TABLE 1 Gene categories and names of differentially expressed genes regulated by miR-27a in Huh-7.5 cells

Protein function and name	Gene	Affy ID[a]	GB acc. no.[b]	Fold change		
				Pre-miR-27a/ miR-control	Anti-miR-27a/ anti-miR-control	Pre-miR-27a/ anti-miR-27a
Cytoskeleton remodeling and Wnt signaling						
Collagen, type IV, alpha 6	*COL4A6*	211473_s_at	U04845	0.85	2.19	2.58
Fibronectin 1	*FN1*	214702_at	AJ276395	0.57	1.14	2.02
Filamin A, alpha	*FLNA*	214752_x_at	AI625550	0.64	1.68	2.61
LIM domain kinase 1	*LIMK1*	204357_s_at	NM_002314	0.67	1.63	2.43
p21/Cdc42/Rac1-activated kinase 1	*PAK1*	230100_x_at	AU147145	0.63	1.58	2.53
Breast cancer anti-estrogen resistance 1	*BCAR1*	232442_at	AU147442	0.96	1.94	2.01
Frizzled homolog 3 (*Drosophila*)	*FZD3*	219683_at	NM_017412	0.51	1.30	2.55
Laminin, alpha 4	*LAMA4*	210990_s_at	U77706	0.63	1.26	2.00
Regulation of lipid metabolism						
CREB binding protein (Rubinstein-Taybi syndrome)	*CREBBP*	235858_at	BF507909	0.54	1.50	2.76
NF-Y	*NF-Y*	228431_at	AL137443	0.41	1.44	3.50
Sterol regulatory element binding transcription factor 2	*SREBF2*	242748_at	AA112403	0.47	1.11	2.35
Membrane-bound transcription factor peptidase, site 2	*MBTPS2*	1554604_at	BC036465	0.50	1.21	2.39
Adenosine A2A receptor signaling						
Mitogen-activated protein kinase kinase 7	*MAP2K7*	226053_at	AI090153	0.90	2.07	2.31
Par-6 partitioning defective 6 homolog beta	*PARD6B*	235165_at	AW151704	0.56	1.35	2.43
Rap guanine nucleotide exchange factor (GEF) 2	*RAPGEF2*	238176_at	T86196	0.46	1.36	2.98
Ribosomal protein S6 kinase, 90kDa, polypeptide 2	*RPS6KA2*	204906_at	BC002363	0.61	1.72	2.83
p53 regulation						
MDM2	*MDM2*	237891_at	AI274906	0.41	1.27	3.07
Ubiquitin B	*UBB*	217144_at	X04801	0.58	1.89	3.24
Promyelocytic leukemia	*PML*	235508_at	AW291023	0.52	1.45	2.80
SMT3 suppressor of mif two 3 homolog 1	*SUMO1*	208762_at	U83117	0.55	1.23	2.22
IL-8 in angiogenesis						
B-cell CLL/lymphoma 10	*BCL10*	1557257_at	AA994334	0.59	1.23	2.08
Janus kinase 2	*JAK2*	205841_at	NM_004972	0.77	1.71	2.23
Sphingosine-1-phosphate receptor 1						
G protein, alpha inhibiting activity polypeptide 2	*GNAI2*	201040_at	NM_002070	0.69	1.49	2.15
G protein, beta polypeptide 4	*GNB4*	223487_x_at	AW504458	0.86	1.78	2.06
Mitogen-activated protein kinase 1	*MAPK1*	1552263_at	NM_138957	0.87	1.93	2.22
GRB2-associated binding protein 1	*GAB1*	226002_at	AK022142	0.66	1.40	2.11

[a] Affy ID, Affymetrix identification number.
[b] GB acc. no., GenBank accession number.

transfection. The efficiency with which these anti-miRNAs inhibit the miRNAs is shown in Fig. 1A. Unexpectedly, inhibition of these miRNAs either had no effect or increased HCV replication in the cases of anti-miR-23a and anti-miR-27a (Fig. 1B).

To investigate the functional relevance of miR-27a in HCV replication in more detail, we evaluated JFH-1 replication in Huh-7.5 cells in which miR-27a was inhibited or overexpressed. The efficacy of miR-27a overexpression is shown in Fig. 1C. Although ectopically introduced pre-miR-27a increased miR-27a levels by approximately 30-fold, the levels of endogenous active Ago2 bound to miR-27a in RNA-induced silencing complexes increased by approximately 5-fold. The RNA and core protein levels of JFH-1 in Huh-7.5 cells decreased to 65% and 40%, respectively, following miR-27a overexpression. In contrast, the RNA and core protein levels of JFH-1 increased by 3- and 1.9-fold, respectively, following miR-27a inhibition (Fig. 1D and E). There was no significant difference in cell viability following miR-27a overexpression or inhibition (Fig. 1D). Furthermore, the rate of Huh-7.5 cell infection by JFH-1 decreased to 35% after the overexpression of miR-27a but increased 4-fold after miR-27a inhibition (Fig. 1F). Thus, miR-27a negatively regulates HCV replication and infection.

miR-27a targets the signaling pathways of cytoskeleton remodeling and lipid metabolism in Huh-7.5 cells. We next examined which signaling pathways were modulated by miR-27a. TargetScan (http://www.targetscan.org/) predicts biological targets of miRNAs by searching for the presence of conserved 8- and 7-mer sites that match the seed region of each miRNA (30). A TargetScan (release 5.2) for miR-27a predicted 921 candidate target genes, and functional gene ontology enrichment analysis of these genes by MetaCore (Thomson Reuters, New York, NY) showed that miR-27a could target the cytoskeleton remodeling and lipid metabolism signaling pathways (data not shown).

To examine whether these signaling pathways were regulated by miR-27a, gene expression profiling was carried out with Huh-7.5 cells in which miR-27a was over- or underexpressed. Transfection of cells with pre-miR-27a and pre-miR-

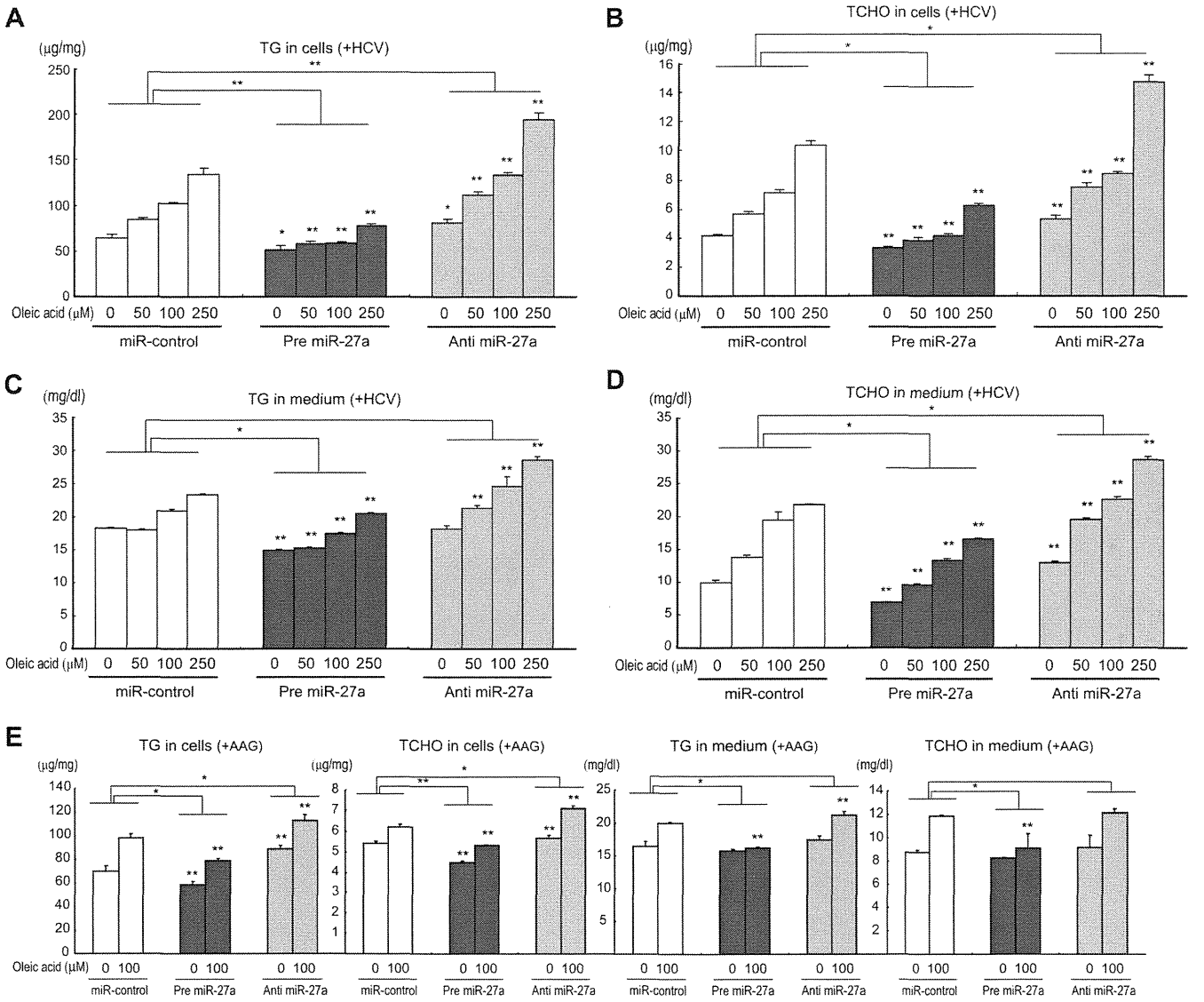

FIG 2 Changes in the lipid contents of Huh-7.5 cells and culture medium caused by pre- and anti-miR-27a. Huh-7.5 cells were transfected with replication-competent HCV RNA (H77Sv2 Gluc2A RNA [+HCV]) or replication-incompetent HCV RNA [H77Sv2 Gluc2A (AAG) (+AAG)] together with pre- or anti-miR-27a. At 24 h posttransfection, increasing amounts of oleic acid (0 to 250 μM) were added to the culture medium, and at 72 h after oleic acid treatment, TG and TCHO levels were measured in the cells and medium. Panels: A, TG in cells; B, TCHO in cells; C, TG in medium; D, TCHO in medium; E, TG and TCHO in cells and medium; A to D, +H77Sv2 Gluc2A (+HCV); E, +H77Sv2 Gluc2A (AAG) (+AAG). Lipid concentration was compared with that of miR-control and pre- or anti-miRNA ($n = 6$). All experiments were performed in duplicate and repeated three times. Values are means ± standard errors. *, $P < 0.01$; **, $P < 0.005$.

control or with anti-miR-27a and anti-miR-control enabled the identification of down- and upregulated genes, respectively. A total of 870 genes were selected with a >2-fold anti-miR-27a/pre-miR-27a expression ratio. Pathway analysis of these genes with MetaCore revealed that they are involved in cytoskeleton remodeling signaling, including that of *COL4A6*, *FN 1*, and *PAK1*; lipid metabolism signaling, including that of *CREBBP* and *SREBF2*; A2A receptor signaling, including that of *RAPGEF2*; and p53 regulation signaling, including that of *MDM2*. These genes were repressed by miR-27a in Huh-7.5 cells (Table 1).

miR-27a reduces TG and TCHO levels in cells and culture medium. Pathway analysis of the gene expression profile regulated by miR-27a in Huh-7.5 cells revealed the presence of many genes involved in lipid metabolism-related signaling pathways. To examine the functional relevance of miR-27a in lipid metabolism, we measured the cellular levels of TG and TCHO in Huh-7.5 cells in which miR-27a was inhibited or overexpressed, respectively. As shown in Fig. 2A and B, TG and TCHO levels in Huh-7.5 cells transfected with miR-control were increased in a dose-dependent manner following the addition of oleic acid (0 to 250 μM). Pre-miR-27a repressed this increase, while anti-miR-27a significantly accelerated it. Similarly, pre-miR-27a repressed the increase in TG and TCHO in the culture medium, while anti-miR-27a significantly accelerated it (Fig. 2C and D).

Similar results were obtained with both HCV-replicating cells

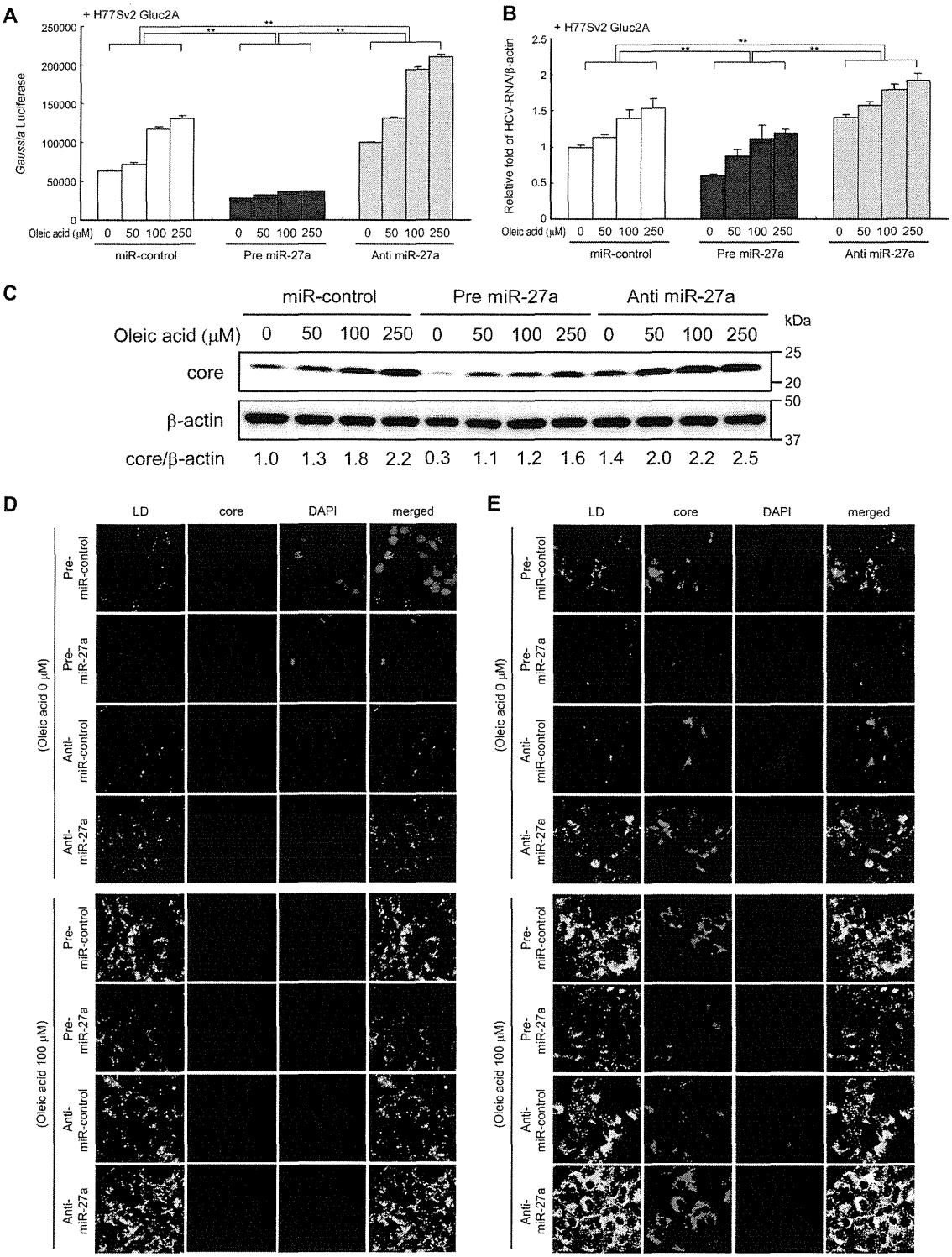

FIG 3 Changes in HCV replication in Huh-7.5 cells caused by pre- and anti-miR-27. Huh-7.5 cells were transfected with H77Sv2 Gluc2A RNA or H77Sv2 Gluc2A (AAG) RNA and pre- or anti-miR-27a. At 24 h posttransfection, increasing amounts of oleic acid (0 to 250 μM) were added to the culture medium. At 72 h after oleic acid treatment, the cells were harvested. (A) Gluc activity in the medium reflecting HCV replication in cells ($n = 6$). (B) Effects of pre- or anti-miR-27 on HCV RNA levels (RTD-PCR, $n = 6$). Experiments were performed in duplicate and repeated three times. Values are means ± standard errors. *, $P < 0.01$; **, $P < 0.005$. (C) Western blotting of HCV core protein in the same experiments. (D and E) Confocal microscopy images of Huh-7.5 cells in the same experiments. D, +H77Sv2 Gluc2A (AAG); E, +H77Sv2 Gluc2A. Cells were fixed, permeabilized, and stained with an anti-HCV core protein antibody. Nuclei were labeled with DAPI. LDs were visualized with BODIPY 493/503 dye. Imaging was performed with a CSU-X1 confocal microscope.

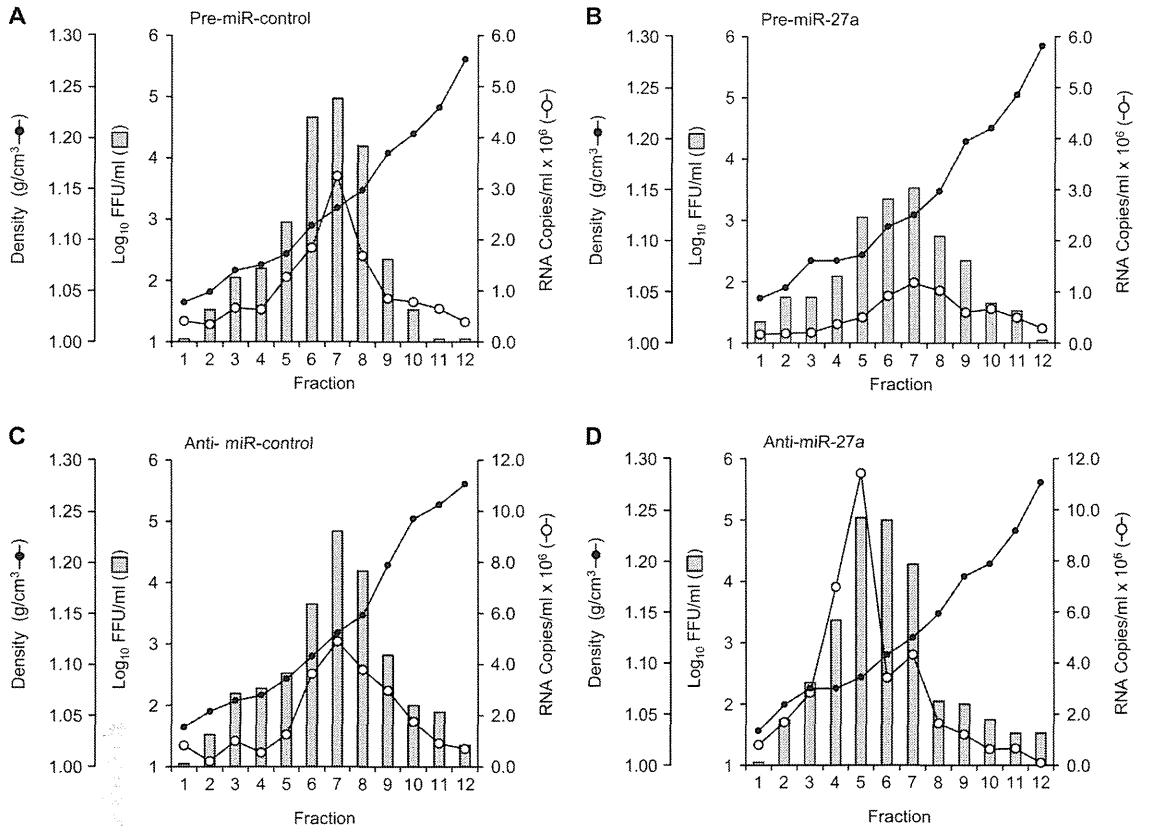

FIG 4 Equilibrium ultracentrifugation of JFH-1 particles in isopycnic iodixanol gradients. Filtered supernatant fluids collected from JFH-1 RNA- and pre- or anti-miRNA-transfected Huh-7.5 cell cultures were concentrated and used to collect fractions (500 μl each). Black circles indicate the gradient densities of the fractions, white circles indicate the HCV RNA titers, and bars indicate HCV infectivity levels. Panels: A, cells overexpressing pre-miR-control; B, cells overexpressing pre-miR-27a; C, cells overexpressing anti-miR-control; D, cells overexpressing anti-miR-27a. Experiments were repeated twice.

(+HCV) (Fig. 2A to D) and non-HCV-replicating cells (+AAG) (Fig. 2E), although the changes in the levels of TG and TCHO in the culture medium were smaller for the non-HCV-replicating cells (+AAG) (Fig. 2E). Correlating with the lipid component findings, replication of the infectious HCV clone H77Sv2 Gluc2A (21), as determined by Gluc activity in the culture medium, and the HCV RNA titer were significantly repressed by pre-miR-27a and increased by anti-miR-27a (Fig. 3A and B). This result was also confirmed by the core protein levels determined by Western blotting (Fig. 3C).

The localization of LDs and core proteins in the cells was visualized by confocal laser microscopy with a lipotropic fluorescent dye and immunostaining of the core protein (Fig. 3E). The LD and core protein levels were substantially repressed by pre-miR-27a and greatly increased by anti-miR-27a antibody. The change in the levels of LDs caused by miR-27a was observed in both HCV-replicating cells (Fig. 3E) and non-HCV-replicating cells (Fig. 3D), although the magnitude of the change was more prominent in HCV-replicating cells.

miR-27a changes the buoyant density and infectivity of HCV particles. The culture medium of Huh-7.5 cells in which JFH-1 was replicating was fractionated by iodixanol gradient centrifugation, and the buoyant density of HCV particles was evaluated (Fig. 4). When the cells were transfected with control miRNA (pre-miR-control and anti-miR-control), the HCV RNA titer (number of copies/ml) and infectivity (number of FFU/ml) peaked at fraction 7 (Fig. 4A and D) and the buoyant density of HCV was estimated at around 1.13 g/cm^3. Transfection with pre-miR-27a did not change the buoyant density of HCV, but it reduced the HCV RNA titer to 0.25-fold of the control and HCV infectivity to 0.024-fold of the control (Fig. 4B). In contrast, transfection with anti-miR-27a reduced the buoyant density of HCV from 1.13 to 1.08 g/cm^3 (Fig. 4B) and increased the HCV RNA titer to 2.1-fold of the control and infectivity to 2.5-fold of the control (Fig. 4C and D). Thus, miR-27a changed the buoyant density and infectivity of HCV.

miR-27a regulates lipid metabolism-related gene expression. The regulation of lipid metabolism-related genes by miR-27a was evaluated in Huh-7.5 cells (Fig. 5 and 6). The lipid synthesis transcription factors PPARγ, FASN, SREBP1, SREBP2, and RXRα were slightly, but significantly, induced in cells in which H77Sv2 Gluc2A replicated. The expression of lipid synthesis transcription factors was compared with that from cells carrying replication-incompetent H77Sv2 Gluc2A (AAG) (Fig. 5 and 6). Unexpectedly, lipid overload with oleic acid had no effect or rather decreased the levels of these transcription factors in non-HCV-replicating cells, probably because of negative feedback mechanisms. Conversely, in HCV-replicating cells, lipid overload with oleic acid further increased the levels of these transcription factors at both the

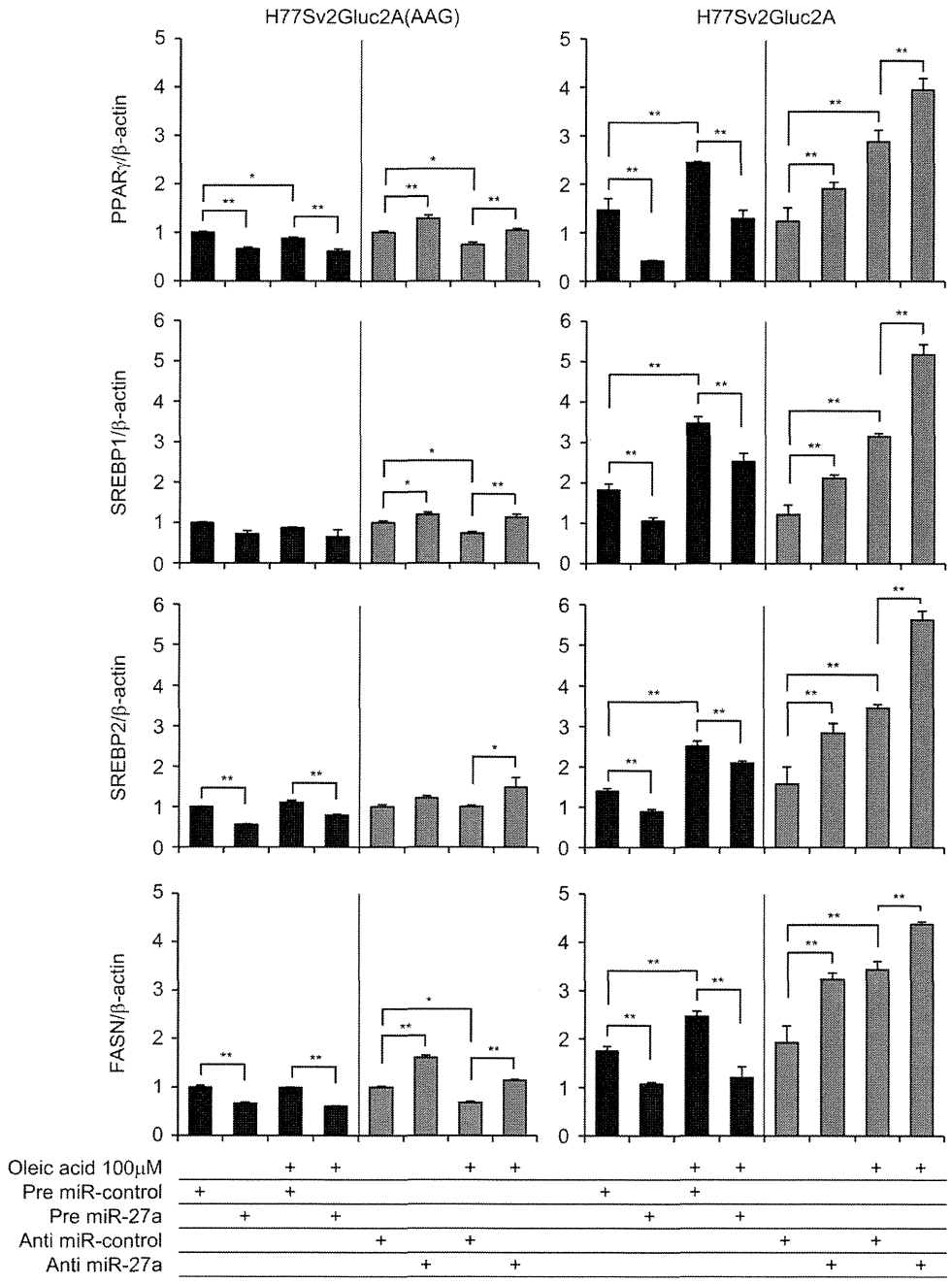

FIG 5 Expression of lipid metabolism-related transcription factors. Huh-7.5 cells were transfected with H77Sv2 Gluc2A RNA or H77Sv2 Gluc2A (AAG) RNA and pre- or anti-miR-27a. At 24 h posttransfection, oleic acid (100 μM) was added to the culture medium, and at 72 h after oleic acid treatment, *PPARγ*, *SREBP1*, *SREBP2*, and *FASN* expression levels were quantified by RTD-PCR ($n = 6$). Experiments were performed in duplicate and repeated three times. Values are means ± standard errors. *, $P < 0.01$; **, $P < 0.005$.

mRNA and protein levels (Fig. 5 and 6A and B). Pre-miR-27a significantly repressed the levels of these transcription factors and, conversely, anti-miR-27a significantly increased their mRNA and protein levels (Fig. 5 and 6A and B). This regulation by miR-27a was observed in both HCV-replicating and non-HCV-replicating cells, although the magnitude of the change was more prominent in HCV-replicating cells (Fig. 5).

As LDs associate with the ER-derived membrane at the site of HCV replication (10) and ER stress was recently shown to promote hepatic lipogenesis and LD formation (31), we next evaluated ER stress markers. Under HCV replication and lipid overload with oleic acid, anti-miR-27a increased the expression of the ER stress markers p-PERK, p-eIF2α, and BiP in Huh-7.5 cells. Conversely, pre-miR-27a significantly decreased the expression of these markers (Fig. 6C). Cell viability decreased after anti-miR-27a transfection and increased following pre-miR-27a treatment (Fig. 6D). Thus, miR-27a repressed the ER stress that was induced by HCV replication and lipid overload.

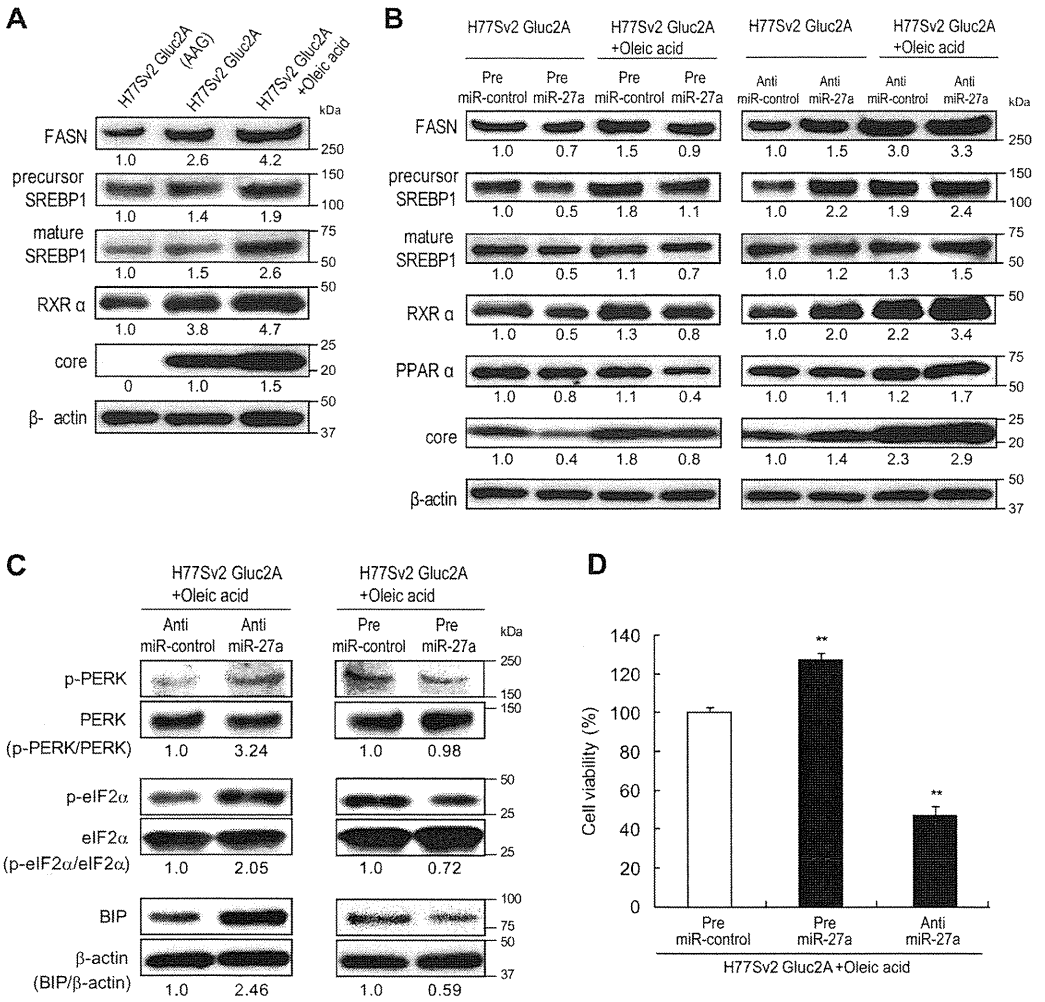

FIG 6 Expression of lipid metabolism-related transcription factors and ER stress-related factors. Huh-7.5 cells were transfected with H77Sv2 Gluc2A RNA or H77Sv2 Gluc2A (AAG) RNA and pre- or anti-miR-27a. At 24 h posttransfection, oleic acid (100 μM) was added to the culture medium. At 72 h after oleic acid treatment, the cells were harvested. (A) Western blotting of lipid metabolism-related transcription factors changed by HCV infection and oleic acid. Experiments were repeated three times. (B) Western blotting of lipid metabolism-related transcription factors changed by pre- or anti-miR-27a. Experiments were repeated three times. (C) Western blotting of ER stress-related transcription factors changed by pre- or anti-miR-27a. Experiments were repeated three times. (D) Cell viability in the same experiments was determined by MTS assay ($n = 9$). Experiments were performed in triplicate and repeated three times. Values are means ± standard errors. *, $P < 0.01$; **, $P < 0.005$.

miR-27a targets RXRα and the ATP-binding cassette transporter ABCA1. We next analyzed the expression of miR-27a target genes. A previous report showed that miR-27a targets RXRα in rat hepatic stellate cells (32), and we confirmed that miR-27a targets the 3′ UTR of human RXRα in Huh-7.5 cells (data not shown). Although the primary sequence of the human RXRα 3′ UTR shares approximately 60% homology with the corresponding rat sequence, the putative miR-27a binding site (ACUGUGAA) is conserved among several different species. Therefore, we constructed an expression vector containing a luciferase (Luc) reporter gene fused to the human RXRα 3′ UTR (pmirGLO-RXRα 3′ UTR) and reevaluated Luc activity (data not shown). Pre-miR-27a repressed Luc activity, while anti-miR-27a significantly increased Luc activity. The introduction of three nucleotide mutations into the conserved miR-27a binding site was shown to abolish these changes in Luc activity. These results confirmed previous findings that miR-27a targets RXRα (32). RXRα interacts with liver X receptor (LXR) and regulates many lipid synthetic genes such as *SREBP1* and *FASN*. We found that the expression of *SREBP1*, *FASN*, and *SREBP2* was regulated by miR-27a (Fig. 6B) and confirmed that *PPARγ* was also regulated by miR-27a, as reported previously (Fig. 5) (33). In addition, *PPARα* was shown to be regulated by miR-27a (Fig. 6B).

We next evaluated the expression of lipid transporter genes. The ATP-binding cassette transporter ABCA1 is mutated in Tangier's disease (34) and plays an important role in the efflux of TCHO for high-density lipoprotein (HDL) synthesis (35). A recent report demonstrated a functional role for ABCA1 in hepatocyte TG secretion to the plasma and in the reduction of cellular TG levels (29). Here we found that pre-miR-27a significantly repressed ABCA1 and, conversely, that anti-miR-27a increased the mRNA and protein levels of ABCA1 (Fig. 7A and B). We identified two miR-27a binding sites (sites 1 and 2) in the 3′ UTR of ABCA1 (Fig. 7C) that were conserved between species (Fig. 7C). An expression vector containing the *luc* reporter gene fused to the human ABCA1 3′ UTR (wild type [WT]) was constructed, and a

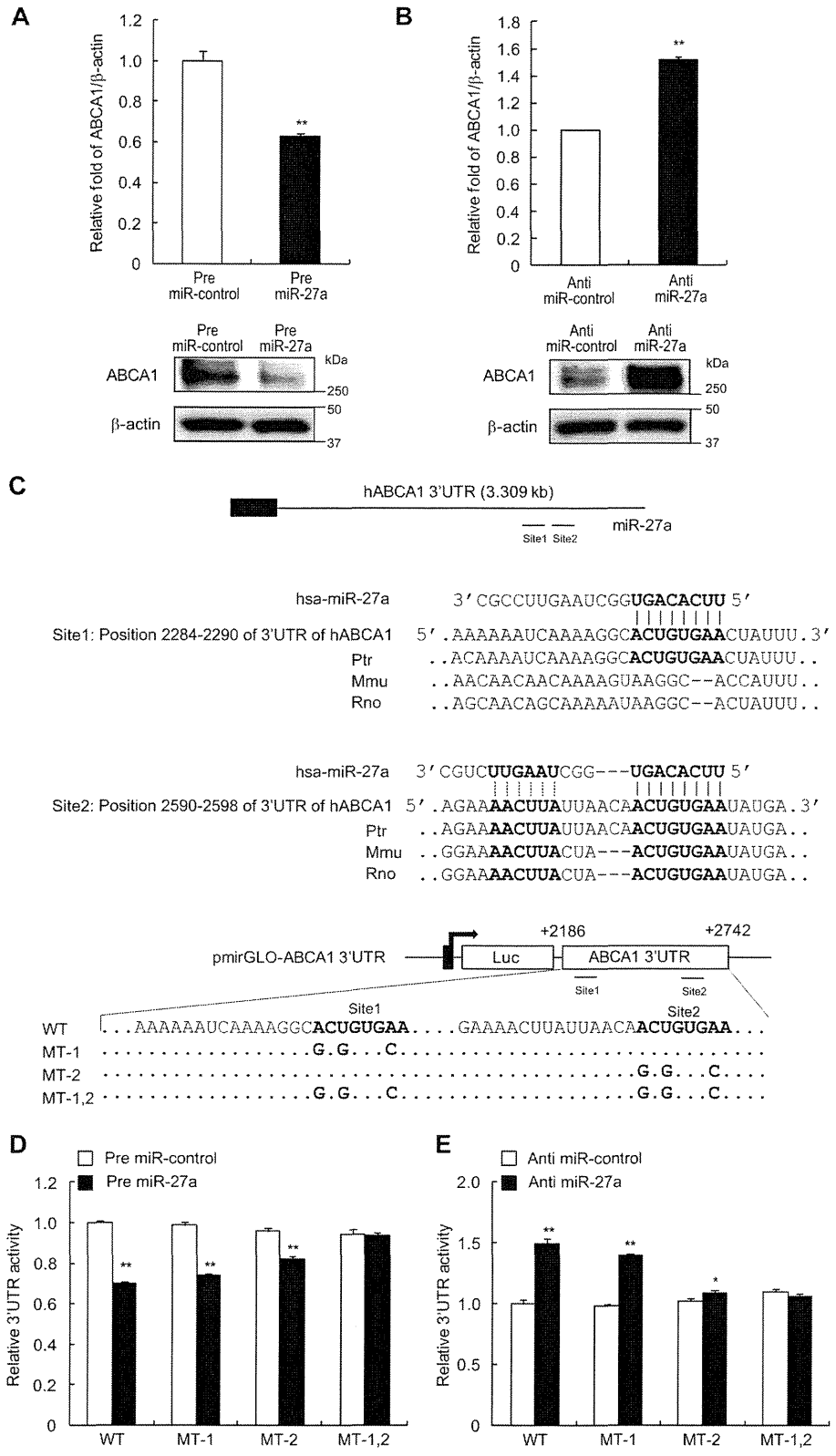

FIG 7 miR-27a targets ABCA1. (A) Regulation of ABCA1 by pre-miR-27a. RTD-PCR and Western blotting of ABCA1 in Huh-7.5 cells at 72 h posttransfection with pre-miR-control and pre-miR-27a ($n = 6$). **, $P < 0.005$. (B) Regulation of ABCA1 by anti-miR-27a. RTD-PCR and Western blotting of ABCA1 in Huh-7.5 cells at 72 h posttransfection with pre-miR-control and anti-miR-27a ($n = 6$). **, $P < 0.005$. (C) Sequence alignment of the ABCA1 3′ UTR and the construction of the luciferase (Luc) expression vector fused to the ABCA1 3′ UTR. Ptr, *Pan troglodytes*; Mmu, *Mus musculus*; Rno, *Rattus norvegicus*; WT, Luc reporter vector with the WT ABCA1 3′ UTR (2186 to 2742); MT-1, Luc reporter vector with the site 1 mutation of the WT; MT-2, Luc reporter vector with the site 2 mutation of the WT; MT-1,2, Luc reporter vector with mutations at sites 1 and 2 of the WT. (D, E) Suppression (D) or induction (E) of Luc activity with the various mutations of the ABCA1 3′ UTR by pre-miR-27a. Huh-7.5 cells were transfected with pre- or anti-miR-control or pre- or anti-miR-27a, and WT, MT-1, MT-2, and MT-1,2. Luc activities were measured at 24 h posttransfection ($n = 6$). All experiments were performed in duplicate and repeated three times. Values are means ± standard errors. *, $P < 0.01$; **, $P < 0.005$.